Automatic classification of vegetation species for climate change analysis by mean of UAV multispectral data.
The case study of two lakes areas in the Maritime Alps.

SAEED HEMMATIANZADEH

A Thesis Submitted in Partial Fulfillment
of the Requirements for the Degree of
Master of Environmental and land engineering

Department of Environmental, Land and Infrastructure Engineering (DIATI)
Politecnico di Torino

Supervised by:
Prof. Francesca Matrone
Eng. Alessandra Spadaro

July 2025

Table of Contents

Abstract

Alpine ecosystems are very responsive to climate change and environmental disturbances, and therefore precise and efficient vegetation surveillance is a key part of ecological research and conservation planning. This thesis describes a multi-source; multi-scale automated land cover and vegetation classification methodology that combines high-resolution UAV-derived multispectral images with medium-resolution Sentinel-2 satellite data. The two target alpine lakes, Lago Vej del Bouc and Lago Brocan, are in the Maritime Alps, and they are used as vegetation change indicators for high-altitude landscapes.

Photogrammetric surveys by UAV in 2024 generated ultra-high-resolution five-band orthophotos in spectral bands RGB, Red, Green, RedEdge, and NIR and were processed in Agisoft Metashape using a band-separate workflow for better spectral matching. Sentinel-2 data for the period from 2017-2024 were, in contrast, analyzed in Google Earth Engine for derivation of NDVI, NDWI, EVI, and SAVI indexes for all seasonal time intervals (June, August, and September), allowing trend as well as large-scale classification analysis.

Object-Based Image Analysis (OBIA) was carried out on eCognition with multi-resolution segmentation, index calculation, and supervised classification. The following machine learning algorithms, Bayesian, Random Forest, Support Vector Machine, K-Nearest neighbors, and Decision Tree, were applied in two classification stages: a primary, general land cover classification (water, soil/rock, vegetation) and, in a subsequent stage, a vegetation type classification with ground-truth data collected in the field.
Bayes classifier outperformed more complex models for all classifications, obtaining highest spatial coherence as well as highest classification accuracy for both levels of classification. UAV images proved more helpful for high-resolution vegetation mapping, but satellite data provided useful temporal continuity in addition to large-area context.

The outcome confirms the efficacy of a dual-scale, object-oriented scheme for simulating highly complex Alpine landscapes. The resulting scheme forms a reusable template for later environmental monitoring and confirms the value of algorithm selection in reaction to complexity in landscapes and data attributes.

1 Introduction

Alpine landscapes constitute among the most environmentally sensitive and ecologically rich regions in the world[1]. Characterized by rugged terrain, short growing seasons, and sharp altitudinal zoning, such landscapes include high endemism and diversity and thus constitute valuable indicators of change in the environment [2]. However, owing to remoteness and logistical challenges involved in conducting fieldwork, overall ecological monitoring in such landscapes proves tricky [3]. Vegetational and aquatic monitoring in alpine areas is central in assessing global warming, land-use change, and glacier recession[4].

Remote sensing methodologies have revolutionized ecological monitoring and analysis [5]. While combining satellite-borne Earth observation and high-resolution UAV (Unmanned Aerial Vehicle) surveys offers an optimal instrument suite for multi-scale monitoring of environments [6]. Sentinel-2 satellite imagery, owing to its ultra-high spatial and temporal resolution, is being applied to large-scale vegetation mappings and hydrological monitoring at an increasing rate [7]. Correspondingly, multispectral equipped UAVs enable ultrahigh spatial detail info and versatility in operation, and thus, are well adapted to localized ecological studies in inaccessibly mountainous terrain [8].

Though large datasets of remote sensing information are available, land cover and vegetation classification effectiveness are primarily dependent on classification algorithm efficiency [9]. In rugged alpine terrain, spectral overlap, shadowing resulting from terrain, and mixed patterns of vegetation complicate traditional pixel-based methodologies [10]. Trying to counter such weaknesses, this study makes use of an object-based image analysis (OBIA) approach and deals with comparative validation among multiple schemes of classification to discern an optimal algorithm that is effective for alpine applications [10].

Key to this thesis is comparative examination among several supervised classification schemes via the eCognition software platform. These include Support Vector Machine (SVM), Random Forest, k-Nearest Neighbors (KNN), Decision Tree, and Bayesian classification [11]. The study puts forward a two-phased classification system: firstly, general classification for large land cover classes (i.e., water bodies, bare ground and rock, vegetated cover) and, in detail, vegetation cover classification via ground truthing during UAV surveys.

As an accompaniment to this classification task, two remote sensing datasets were used. In consideration of the satellite component, Sentinel-2 images with minimum cloud cover were selectively hand-picked from the Copernicus Open Access Hub, during July, August, and September 2017 to 2024. The images were selected for good observations of both study lakes, Lago Vej del Bouc and Lago Brocan. Google Earth Engine (GEE) was used to filter and download these images through their permanent identifiers. NDVI and NDWI spectral indices were calculated [12], and supervised classification was applied to categorize water, soil/rock, and vegetation cover.

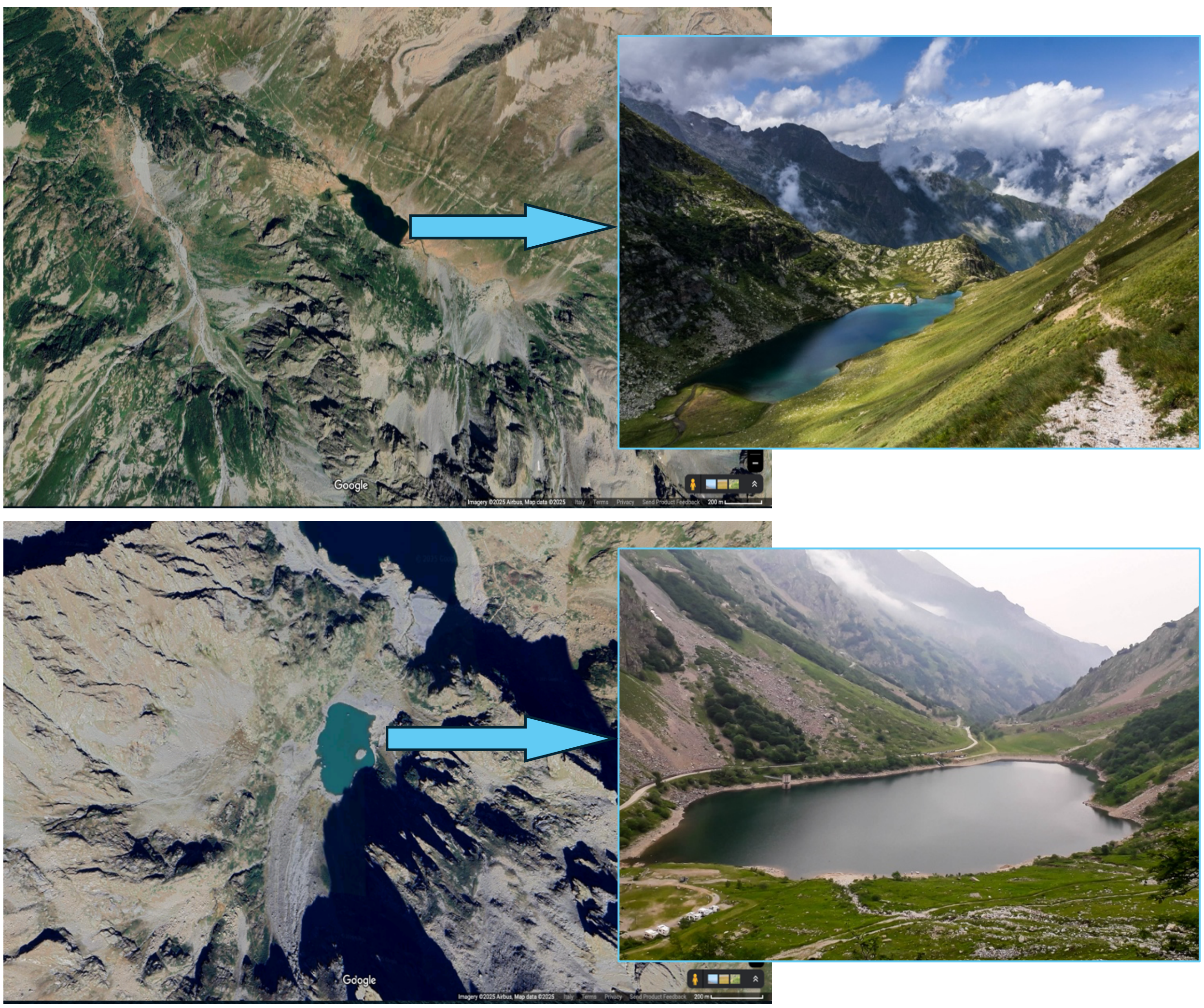

Figure 1- Geografical location of 2 Aline lakes(Up:Lago vej del bouc, Down: Lago Brocan)

For the UAV component, a multispectral survey conducted in July 2024, by the Geomatics Laboratory, Politecnico di Torino, provided high-resolution images for both lakes. Preliminary processing, which had been completed in DJI Terra software, was replaced by Agisoft Metashape due to quality issues. After an experiment with single-chunk processing, it was optimized to divide multispectral bands in five chunks (RGB, Red, Green, RedEdge, and NIR) separate, allowing for separate orthophotos for each band in each lake. This optimized this process to refine geometric accuracy and minimize co-registration errors, achieving an eventual positional accuracy under 3 cm. These orthophotos were then transferred in eCognition for classification using multiple AI and ML algorithms.

By integrating medium-resolution satellite imagery and high-resolution UAV data and employing a comparative, AI-classification method, this dissertation aims to provide a transferable approach to monitoring vulnerable alpine ecosystems. The article belongs to a growing body of literature on adapting to climatic change, conserving natural diversity, and managing environmental resources in mountain environments. Furthermore, it uncovers a crucial new finding in terms of classifier selection in deriving valid land cover estimates, specifically in mixed scenarios where remote sensing is becoming ever more central to environmental inquiry.

1.1 ACLIMO Project

This work is part of a research partnership between the Politecnico di Torino and Management Authority of Protected Areas of the Maritime Alps (APAM), in the framework of the France–Italy ALCOTRA (Alpi Latine COoperazione TRAnsfrontaliera) 2021–2027. The partnership of this cross-border cooperation project includes several Italian and French parks and institutions: Parco Nazionale del Mercantour, APAM, Parc National des Écrins, Authority of Management of the Parks of the Cottian Alps, Parc National de la Vanoise, Gran Paradiso National Park, Ente of the Ligurian Alps Regional Nature Park and the City of Cuneo.

The overall aim of this collaboration is the study on the impact of the climate change on mountain ecosystems in the Maritime Alps Park, focusing on glaciers, forests, grassland peatlands, wetland and water resources. Second, the project will provide support for land management through detection of the risk and vulnerability situation and predictions of possible future developments.

The approach relies on a multi-platform, multi-sensor, and multi-scale framework, organized in three observations scales: small, medium, and large (Fig. 2).

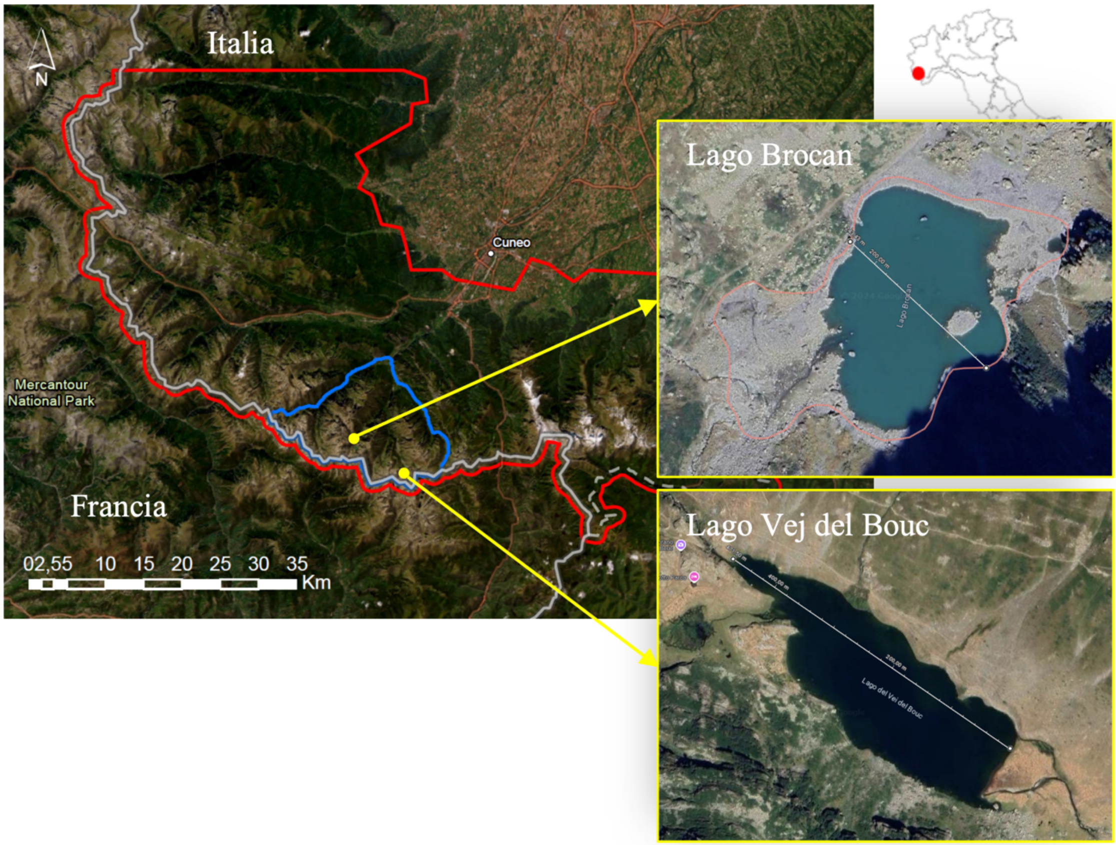

Figure 2-Area of interest at small scale (red) and medium scale (blue), and lakes analyzed at large scale (yellow).

Environmental monitoring and decision making in APAM are based on a standardized procedure using solid, and well-documented algorithms. On a fine scale, satellite images are analyzed to identify long-term developments within the study area. Particularly, developments on snow cover, vegetation, land use and the water level of alpine lakes are analyzed. "The Copernicus Land Monitoring Service (CLMS) with data from the Landsat and Sentinel satellite constellations that reaches back 20–25 years. We focus on imagery from April (usually representing maximum snow cover by ARPA Piemonte), June (maximum vegetation and lake water extent), and August (for remaining snowfield and late-summer water extent). Such land cover dynamics are cross correlated with meteorological data collected at ARPA Piemonte weather stations, validating also indirectly remotely estimated environmental parameters.

In the medium scale attention is given to vegetation, wetlands and glaciers. Photogrammetric data (preferably multispectral) is used to generate high resolution land cover classification map more detailed than existing maps like Corine Land Cover. The classification may utilize automated or semi-automated methodologies which may involve AI and deep learning models. On the large scale (i.e., centimeter-level feature detail and geometric precision), two alpines lakes (Lago

Brocan and Lago Vej del Bouc) represent sentinel sites for climate change modeling. These lakes were mapped with bathymetric sensors and drones carrying RGB and multispectral cameras. An AI-based image analysis was performed using UAV aerial imagery allowing for an automatic recognition of features (e.g., invasive herbaceous or shrub species) and reconstruction of lake bathymetry in littoral zone. Table 1 lists the sensors, and data used.
Photogrammetric flights with the UAV were carried out in the alpine lakes in July and October 2024 (in this thesis only July project have been analyzed) using a DJI Mavic 3M equipped with an RTK module. 6,116 images were acquired for Lago Brocan and 4,947 for Lago Vej del Bouc. The first step in processing in DJI Terra produced dense point clouds with a total of 28.1 and 32.5 million points for Vej del Bouc and Brocan, respectively. These reconstructions had an RMSE (Root Mean Square Error) between 2 and 3 cm, with 7 ground control points (GCPs) for Vej del Bouc and 18 for Brocan.

Table 1- List of sensors and datasets

Small scale	Sentinel-2 Sattelite **Images from the months of April, June, and August (2017–2024)** **Spatial resolution: 10 m** **Spectral resolution: 13 bands**
Large scale	**DJI Mavic 3M**  GNSS RTK, 5 sensors, RGB 4/3 (17.3 × 13 mm), 20 MP, 5280 × 3956, Pixel size: 3.3 × 3.3 µm Focal length: 13 mm, Multispectral 1/2.8", 6.058 × 4.415 mm, 5 MP, 2592 × 1944 Bands: Green (G): 560 ± 16 nm, Red (R): 650 ± 16 nm, Red Edge (RE): 730 ± 16 nm, Near-Infrared (NIR): 860 ± 26 nm Weight: 951 g

1.2 Objectives

The main goal of this thesis is to establish an efficient and effective method for mapping alpine vegetation types and canopy land cover classes as derived from medium resolution Sentinel-2 data combined with high-resolution UAV multispectral data. The study centers on two high mountain lakes (Lago Vej del Bouc and Lago Brocan) in the Maritime Alps, with the aim of producing fine resolution maps of vegetation with the purpose of being employed for climate change analyses and environmental monitoring.

The comparative assessment among various supervised classification algorithms associated with eCognition software environment constitutes an essential contribution of this research. The algorithms evaluated are Support Vector Machine (SVM), k-Nearest Neighbors (KNN), Decision Tree, Random Forests, and Bayesian classification. Analogously, on the basis of a systematic experiments, the Bayesian classifier always gave the best accuracy, in particular in complex and mixed vegetation areas. This result emphasizes the appropriateness of the algorithm to alpine conditions, where spectral ambiguity and topographic variation commonly create problems for classic classification methods.

This study uses the two-step classification system. The classification process proceeds into separate phases, in the first phase, big land cover elements such as water body, bare soil and rock, and vegetated areas, are classified with the use of UAV orthophotos. These orthophotos were derived from an improved photogrammetric workflow developed in Agisoft Metashape, with all the multispectral bands (RGB, Red, Green, Near Infrared, RedEdge) processed independently to avoid co-registration errors. This process yielded five orthophotos per lake at a spatial resolution of less than 3 cm, providing high geometric accuracy. In the second stage, the vegetated areas are presented by the first classification are further processed to an identifiable type of a vegetation. This higher taxonomic level is the result of field-validated ground-truth samples acquired during UAV campaigns in July 2024 and provide more detail on the alpine vegetation composition.

Sentinel-2 imagery was used for temporal and spatial context as a complement to the UAV analysis. July, August, and September images of 2017–2024 were chosen manually from the Copernicus Open Access Hub, considering a minimal number of clouds and the representation of both lakes. These images were analyzed in GEE and employed with atmospheric correction, cloud screening and spatial cropping. The principal vegetation and water indices (NDVI, SAVI, EVI, and NDWI) were computed, and supervised classifications were carried out using Random Forest classifier. The satellite-based classification facilitated detection of the temporal trends and validation UAV-based classification results.

All classification results were assessed following accuracy-based measures, such as the overall accuracy, kappa coefficient, precision, recall, F1-score. Confusion metrics were compiled with reference to 'ground-truth' data, and classifier performance was measured on both spatial scales and data sources.

Finally, this study seeks to contribute not only to improved accuracy of alpine vegetation mapping, but also to a better understanding regarding the performance of the most popular classification methods in object-based modeling of alpine areas. The approach developed here is scalable and flexible, and thus widely applicable, offering a useful tool for ecological monitoring, water resources management and climate adaptation in mountain contexts.

2 Literature review

The correct identification of vegetation in alpine habitats is a difficult task because the floras in these environments are complex and the topography varies widely [13]. This thesis deals with this problem by combining Sentinel-2 satellite imagery, UAV-based remote sensing in multispectral data and cutting-edge classifiers based on artificial intelligence (AI) and machine learning (ML). High-altitude habitats are particularly vulnerable to changes in climate and environmental stress notably because of the presence of species adapted to extreme ecological niches, that are found nowhere else but there, and that need to be monitored to get reliable ecological assessment (conservation planning, impacts of climate change)[14].

However, traditional methods of classification have restrictions under such condition. The spectral responses of the various vegetation types typically overlap, the landscape is very heterogenous, and both the resolution in space and wavelengths of the available instruments may not be sufficient to resolve densely packed vegetation at the fine resolution of the SEN2image [15], [16].

Spectral indices such as the Normalized Difference Vegetation Index (NDVI) [17]and the Normalized Difference Water Index (NDWI) [18] have already been applied to vegetation and hydrological study. However, these indices alone often do not represent the structural and spectral heterogeneity encountered in alpine vegetation, particularly in mixed land-cover and high-relief regions [11]. Although satellite data have been useful for large area environmental analysis, there are few successful cases in combining UAV-based high-resolution multispectral data with the method of machine-learning algorithm for improving the classification accuracy in alpine area[19], [20]. This clearly demonstrates a significant methodological missing link and the increasing relevance of combined approaches combining several data sources with strong classification methods.

In order to deal with these, a multisource and multimethod classification framework is proposed in this thesis, exploiting the complementary information between Sentinel-2 and UAV image data. Sentinel-2 imagery is employed for the purpose of long-term temporal investigation and the realization of regional coverage, while UAV imagery supports object-based detailed classification on finer spatial scales. One of the main features of this work is the systematic comparison between five supervised classification algorithms: Support Vector Machine (SVM), k-Nearest Neighbors (KNN), Decision Tree, Random Forest and Bayesian classification. These models were realized in the eCognition software system, which employs the object-based image analysis (OBIA) concept to combine spectral, spatial, and contextual properties at the level of image segments, and in doing so surmounts a range of shortcomings associated with pixel-based methods [10].

This is why Random Forest and SVM have been the most popular classifiers for remote sensing applications as, amongst other reasons, these classifiers are suitable for: I) high-dimensional data, and II) non-linear class boundaries [21], [22]. Nonetheless, in the context of alpine vegetation mapping, the Bayesian classifier in this study performed better than the other models. Although not as often employed nowadays in the literature, the Bayesian approach was found to be solid and accurate in its functioning, especially when combined with OBIA and multispectral UAV images. Its statistical nature, capability to describe class distributions, and flexibility with restricted training data render it suitable for models of spectral blur and inhomogeneous vegetations [23].

Table 2-Comparative Summary of Classification Algorithms in Remote Sensing

Classifier	Key Features	Advantages (Pros)	Limitations (Cons)
Bayesian	Probabilistic model based on class-conditional distributions.	- Simple and fast - Works well with small datasets - Effective in OBIA with homogenous segments	- Assumes feature independence - May underperform on highly complex, high-dimensional data
SVM	Maximizes margin between classes using support vectors.	- High accuracy with small training sets - Good with high-dimensional data - Robust to overfitting	- Sensitive to kernel choice- Computationally intensive with large datasets
KNN	Classifies based on majority vote among nearest neighbors.	- Easy to implement- No training phase- Effective in low-noise data	- Sensitive to outliers - Requires large memory - Slower with big datasets
Random Tree	Single decision tree built from random feature splits.	- Fast training - Easy to interpret - Handles categorical and numerical data	- Prone to overfitting - Lower accuracy compared to ensembles
Random Forest	Ensemble of decision trees with random sampling and feature selection.	- High accuracy - Robust to noise and overfitting - Handles large datasets well	- Complex to interpret - Slower than single-tree models - May require parameter tuning

These results are consistent with earlier findings indicating that the performance of an algorithm is based on technical complexity as well as how well the algorithm fits the data and landscape. To take advantage of this, the strength of the OBIA framework of eCognition is that contextual features such as texture, shape and object size are used to refine classification accuracy, which contributes to improve the performance of the Bayesian classifier. Therefore, this study provides further evidence for Bayesian methods and advocate its use for wider implementation in object-based remote sensing applications.

2.1 Automatic Classification of Vegetation

The automatic categorization of alpine vegetation is an important task in environmental monitoring since alpine ecosystems are very sensitive to climate changes and frequently disturbed by human activities. Mountain areas with their steep topography, altitudinal diversity and high biodiversity can be expected to be especially sensitive to climate change. The response of vegetation in these environments is a good indicator of global environmental change [14]. Despite of this, particularly the mapping and classification of vegetation is challenging in those regions as a result of dense land cover, less availability of ground-truth data, and instinct spectral signals considered there by many plant species very similar.

Remote sensing has proven to be an effective solution for these problems, providing repeatable observations of widespread and frequently difficult to access terrain. Among the satellite platforms available, the Sentinel-2 is particularly useful thanks to its high spatial, spectral and temporal resolution, enabling the monitoring of land cover and vegetation dynamics at fine scale [7]. It still becomes inaccurate, despite the improvement of classification by remote sensing, the classification of alpine vegetation based on satellite imagery suffers from chronic inadequacy, particularly because of the spectral interference among vegetation types and the spatial heterogeneity of mountain terrain [11]. This situation often results in classification errors and lack of confidence in vegetation maps.

Environmental remote sensing has seen a surge in the popularity of Unmanned Aerial Vehicles (UAVs) for achieving higher classification accuracy. With both multispectral and hyperspectral sensors, UAVs get ultra-high-resolution images that can see fine-scale spatial and structural variation in what vegetation makes up a particular patch details that can escape satellite sensors. The capability to fly at low altitudes and with flight paths that can be tailored to the feature being surveyed means that UAVs are especially well suited to texture rugged or steep terrain to produce localized data, which is both detailed and consistent through space [24]. When integrated with remote sensing data from satellites, these poly-source datasets increase the strength and the comprehensiveness of vegetation mapping by covering space in between regional patterns and small-scale ecology [14].

Recent research has revealed that the combination of UAV imagery and sophisticated machine learning techniques have proven to be more beneficial. Significant improvement over pixel-based classification methods was also reported by Belgiu and Drăguţ [11] using Random Forest classifiers in the application of Sentinel-2 data. Similarly, Huang et al. [19] found that integrating UAV and Sentinel-2 data enhanced the classification accuracy in rugged mountainous terrains. Despite these encouraging results, a large proportion of previous work has simply analyzed satellite or UAV data independently of the other type of image and has not exploited the synergies between the two image types.

The objective of this thesis is to fill this gap by developing an integrated classification framework with the combination of Sentinel-2 satellite imagery and few available UAV-based multispectral data. The approach uses machine learners such as Random Forest and other machine learning techniques to improve classification performance. This multi-source, multi-resolution method is especially important for alpine regions, where spatial heterogeneity and sparse in-situ measurements often restrict the application of traditional remote sensing techniques.

In addition to higher spatial resolution, advances in UAV technology have recently made it possible for more accurate vegetation classification. High-resolution multispectral and hyperspectral UAV data can detect fine scale differences in vegetation condition, composition and structure. Fusing UAV-based hyperspectral data and Light Detection and Ranging (LiDAR) has demonstrated a greater potential for species-level classification as it offers both spectral and structural information [16]. In addition, texture features and spatial variability metrics derived from UAVs can increase the classification accuracy of vegetation types, particularly for mixed-species cover [25]. Another study has successfully employed Multiview Hyperspectral Data acquired with UAV toward classification of vegetation species as a result of slight spectral diversity [20]. These findings demonstrate the transformative power of the UAV-based remote sensing for accurate, fine-resolution vegetation mapping in the ecologically sensitive alpine landscape.

2.2 Spectral Indices for Vegetation Classification

Spectral indices are algebraic functions of reflectance values in isolated spectral bands that maximize the observation and analysis of unique land surface characteristics, particularly vegetation. Spectral indices are also widely embraced in remote sensing as they can utilize the special spectral properties of vegetation, mainly the high absorption in the red spectral region due to chlorophyll and the high reflection in the near-infrared (NIR) band as a result of the internal structure of the cells within the leaves [26].

One of the most commonly used spectral indexes is the Normalized Difference Vegetation Index developed by [17]. NDVI can be computed as:

$$\mathrm{NDVI} = \frac{(NIR - RED)}{(NIR + RED)}$$

NDVI has the advantages of its ease of application, scalability, and high relationship with vegetation health and density. NDVI, however, is affected by a series of confounding factors, such as the influence of the background reflectance of the landscape, the atmospheric environment, and the calibration errors of the sensor, which can limit its usefulness in complex cases in mountain environments [27], [28].

In order to address some of these problems, Huete (1988) introduced the SAVI. SAVI incorporates a soil brightness correction factor (L) in the NDVI equation:

$$\mathrm{SAVI} = \frac{(NIR - RED)}{(NIR + RED + L)} \times (1 + L)$$

The standard value of L is 0.5, corresponding to intermediate vegetation cover. SAVI efficiently eliminates the effect of the soil noise, making it very suitable in arid and semi-arid environments or other low-density vegetations. However, the appropriate determination of the L factor is necessary based on vegetation cover and terrain characteristics, and errant estimation can impair classification accuracy [27].

Enhanced Vegetation Index (EVI) has been developed to better address vegetation monitoring, particularly in regions in which NDVI saturates, i.e., dense forests. EVI utilizes a more advanced formula:

$$\mathrm{EVI} = 2.5 \times \frac{(NIR - RED)}{(\mathrm{NIR} + 6 \times \mathrm{Red} - 7.5 \times \mathrm{Blue} + 1)}$$

Adding the blue band to correct for atmospherically induced problems and normalizing for background reflectance, EVI enhances sensitivity to canopy structure and minimizes the atmospheric distortion effect. Yet, its reliance on the blue band restricts its use to all sensor platforms and may be unsuitable in sparse cover or arid regions [28].

Though developed to identify open water bodies, the Normalized Difference Water Index (NDWI) of McFeeters (1996) has also gained application in the study of vegetation, particularly in the determination of the water content of plants. NDWI can be computed as:

$$\mathrm{NDWI} = \frac{(\mathrm{GREEN} - NIR)}{(\mathrm{GREEN} + NIR)}$$

Utilizing the low water reflectance in the NIR band and increased reflectance in the green band, NDWI is not an index of vegetation per se, yet can prove valuable when examining vegetation stress and hydrological regimes, especially in alpine environments, as moisture availability profoundly influences the dynamics of such vegetation. However, NDWI may incorrectly mislabel wet vegetation as water and is best used as a supporting index [29].

In a complex environment like alpine settings, where vegetation is sparse, patchy, and strongly driven by moisture gradients, topography, and the seasonal snowmelt, a single index cannot sufficiently account for the entire variability of the vegetation. Belgiu and Drăguţ (2016) [11] proved that a fusion of indices and machine learning algorithms, such as Random Forest (RF), increases the classification accuracy in mixed land cover types. Similarly, Xue & Su (2017)[30], who showed that EVI is superior to NDVI in dense canopies, while SAVI provides better discrimination in sparser vegetation zones, suggesting that index selection should be adjusted according to environmental background.

A promising strategy for improving vegetation classification involves index stacking, where several spectral indices (e.g., NDVI, SAVI, EVI, NDWI) are used as layers in supervised classification models. This approach enhances feature space separability and provides a more nuanced representation of vegetation characteristics [31]. Moreover, integrating indices derived from both UAV and satellite sensors (such as Sentinel-2) allows for the exploitation of their respective advantages high spatial resolution from UAVs and high spectral diversity from satellites [32].

Although useful, spectral indices are subject to a range of limitations. Topographic effects can greatly alter the reflectance value in mountain regions because of the variable sun-slope angles and orientations. Topographic correction using the Minnaert correction or the C-correction is necessary to minimize these effects [33]. Sensor variation is another one; spatial, spectral, and radiometric differences can cause inconsistencies in the performance of the indices. Sentinel-2, for example, has incorporated red-edge bands that are helpful for the monitoring of vegetation, whereas UAV-based RGB sensors might not be able to do the same [15].

Phenological variation also makes vegetation classification more difficult, as leaf area, pigment concentration, and water content change seasonally. The distinction among phenological phases and long-term vegetation directions may necessitate multi-temporal analysis[34]. Last, atmospheric disturbance and background soil reflectance are continuing challenges to all spectral indices. Atmospheric correction (e.g., Sen2Cor for Sentinel-2 images) and surface reflectance retrieval as a preprocessing step are necessary to reduce these influences.

Finally, spectral indices are very useful for vegetation classification in the case of remote sensing. NDVI, SAVI, EVI, and NDWI all bring unique strengths to the table that, in combination, allow for a more robust and accurate evaluation of vegetation characteristics. Specifically, in the case of complex alpine ecosystems, a multi-index, multi-source approach (aided by advanced classification methods) provides a holistic framework for precise and meaningful vegetation mapping. Such a methodology is followed by the current study, taking advantage of the potential of UAV and Sentinel-2 data synergy, in an attempt to meet the peculiar challenges of vegetation classification in alpine environments and enhance the readability and accuracy of land cover estimates.

2.3 Using AI and Machine Learning Algorithms

In the past few years, the efforts to incorporate AI and ML techniques have led to tremendous progress in the classification of vegetation and land cover using RS imagery. Pixel-based (or threshold-based) approaches, which are conventional and basic methods (because they appeared in the 70s and 80s), usually do not provide good performance in heterogeneous environments where spectral signals have mixed together as a result of topography, atmospheric effects, or in-between land cover zones.

In comparison to mechanistic models, AI-driven techniques are able to encapsulate intricate dynamics or non-linearities from datasets of high dimensionality, which can provide higher accuracy and flexibility across various landscape heterogeneities [35].

Support Vector Machines (SVM) and Random Forests (RF) are significantly popular among the ML methodologies for remote sensing, as they are robust, non-parametric, and have the capacity to address noisy, high-dimensional inputs [11], [21]. RF, proposed by Breiman (2001) [22], is an ensemble of decision trees trained with bootstrapped subsets of the samples using randomly chosen features, to prevent overfitting and enhance generalization. The SVM, however, is known to be highly effective in separating classes in a complex feature space and is well suited when the amount of training data is small, but the classes are well separated [36].

More recently, deep learning, especially Convolutional Neural Network (CNN) features, has been focused on serving as end-to-end feature extractors to jointly learn spatial and spectral features of the image data under investigation [37], [38]. CNNs are particularly beneficial in tasks where texture and context are important, such as vegetation mapping. Yet, they are not readily applicable in alpine or remote sites where large amounts of annotated training data and access to high-performance computing systems are not available [39].

To tackle these challenges, in this paper we focus on the role of interpretable and accessible ML (machine learning) classifiers in the context of object-based image analysis (OBIA) and how these classifiers are used in eCognition software. Contrary to pixel-based approaches, OBIA exploits spatial, spectral, and contextual information at the segment level, thus being suitable for the elaboration of high-resolution UAV orthophotos of a complex mountain environment.

The workflow comprises first an object-based segmentation of imagery in the UAV image segmentary, where we extract features in the shape of RGB (Red, Green, Blue), NIR (Near-infrared), RedEdge, Green, Red and classify these into the main land cover classes: water, exposed soil/rock, and vegetation. A second phase of the classification separates the vegetational types with ground-truth field information.

Classifier performance was tested by applying 5 supervised ML algorithms (Random Forest, Support Vector Machine, k-Nearest Neighbors [KNN], Decision Tree, and Bayesian classification) to the same object-based inputs. Although RF and SVM performed well, the Bayesian classifier not only achieved the best classification accuracy, but also the highest-class purity and spatial coherence. This finding supports the idea according to which, within OBIA workflows, where spatial and contextual models are naturally represented, more elementary probabilistic classifiers could be stronger than more sophisticated ensemble or kernel designs.

Satellite (and UAV) imagery was processed in Google Earth Engine (GEE), providing online capacity for large-scale data processing, atmospheric correction, and vegetation index calculation. The scalable infrastructure of GEE and the object-based analytical tools of eCognition delivered a strong and adaptable pipeline for vegetation classification in difficult landscape contexts.

These results highlight the need for a data-adaptive choice of a classifier. In the rugged terrain of the mountains, ground-truth data are generally under-sampled, and landscape heterogeneity can be high; therefore, simpler, more transparent classifiers such as Bayesian classifiers may be more robust than computationally intensive classifiers. Furthermore, the OBIA method emphasizes the role of spatial context and quality of segmentation in improving classification accuracy.

New trends in remote sensing indicate that fusion, hybrid, and ensemble methods could lead to greater enhancements. For instance, CNNs may act as feature extractors, and the outputs may be fed into a classical classifier such as RF or SVM to make the final decision [40]. Transfer learning is also a promising approach, as it allows scientists to fine-tune pre-trained models (e.g., ImageNet or BigEarthNet) to a study area at low training cost while improving generalization.

However, there are some limitations. The most important one is the need for annotated high-quality data, and this is even harder to find in alpine environments. Further, the computational complexity and restricted interpretability of DNN models make them challenging to deploy for ecological and decision-maker applications. A surge in interest in Explainable AI (XAI) is testament to the change in attitudes towards transparency and interpretability in complex models.

In summary, this research has supported the use of interpretable machine learning classifiers in an object-based framework, with GEE preprocessing, for remote sensing applications. The results demonstrate that simple Bayesian classification, in combination with extensive data segmentation and data fusion together with the use of multiple sources, can outperform complex classifiers in certain ecological scenarios. The approach allows scalable and customizable high-resolution vegetation mapping in alpine and comparable settings.

3 Methodology

In this study, we applied a systematic approach including satellite imagery, UAV imagery, remote-sensing indices, and state-of-the-art machine-learning (ML) algorithms to classify alpine vegetation. The aim was to design a general classification framework with high accuracy and generalization capability in the presence of the complexity of diverse mountainous areas.

Classification of alpine areas using remote sensing faces the advantages and obstacles of having variable vegetation and topographical composition, and changes throughout the seasons. To counterbalance these complexities, we combined Sentinel-2 data with UAV-based high-resolution orthophotos, which capitalize on the spatial and spectral-resolution synergy of both data types. The rationale for applying this multi-source method is that it may enhance spatial detail and spectral diversity, which can be crucial for discerning fine-scale vegetation classes that are common in alpine terrain.

The research involved a methodological pipeline that comprised the following steps sequentially: data collection, preprocessing, spectral-index generation, segmentation, feature extraction, model training, classification, and accuracy evaluation. Sentinel-2 imagery was preprocessed to Level-2A surface reflectance with the processor Sen2Cor, and UAV images were orthorectified and mosaicked with Agisoft Metashape. Terrain correction was performed by means of a high-resolution Digital Elevation Model (DEM) to reduce the influence of topography. These preprocessing stages retained the geometric and radiometric quality of the input images.

A special effort was made to define the suitable periods (July 2024) for the description of phenological variation. Furthermore, a number of vegetation and water indices (i.e., NDVI, NDWI) were computed to enhance the feature space. Image objects were subsequently developed from the images based on multiresolution segmentation within eCognition to alleviate some of the pixel-based effect associated with classifications. These segments were used for retrieving statistical, textural, and contextual features for the purpose of vegetation classification.

For the purpose of methodological rigor, we chose Random Forest (RF), Support Vector Machine (SVM), Bayesian, k-Nearest Neighbors (KNN), and other algorithms as the traditional machine-learning classifiers. These choices were justified by the literature, according to which these techniques have proved to achieve good performance in vegetation classification [11], [37]. The RF model was programmed using scikit-learn in the Python language, and the corresponding hyperparameters were fine-tuned by grid-search 10-fold cross-validation.

RF and SVM were especially efficient for high-dimensional feature spaces and modeling non-linear relationships between input variables. To evaluate the performance of each of the models, accuracy measures such as overall accuracy, kappa coefficient, precision, recall, and F1-score were generated. The confusion matrices and variable-importance plots were also examined to better understand the behavior of the classifiers.

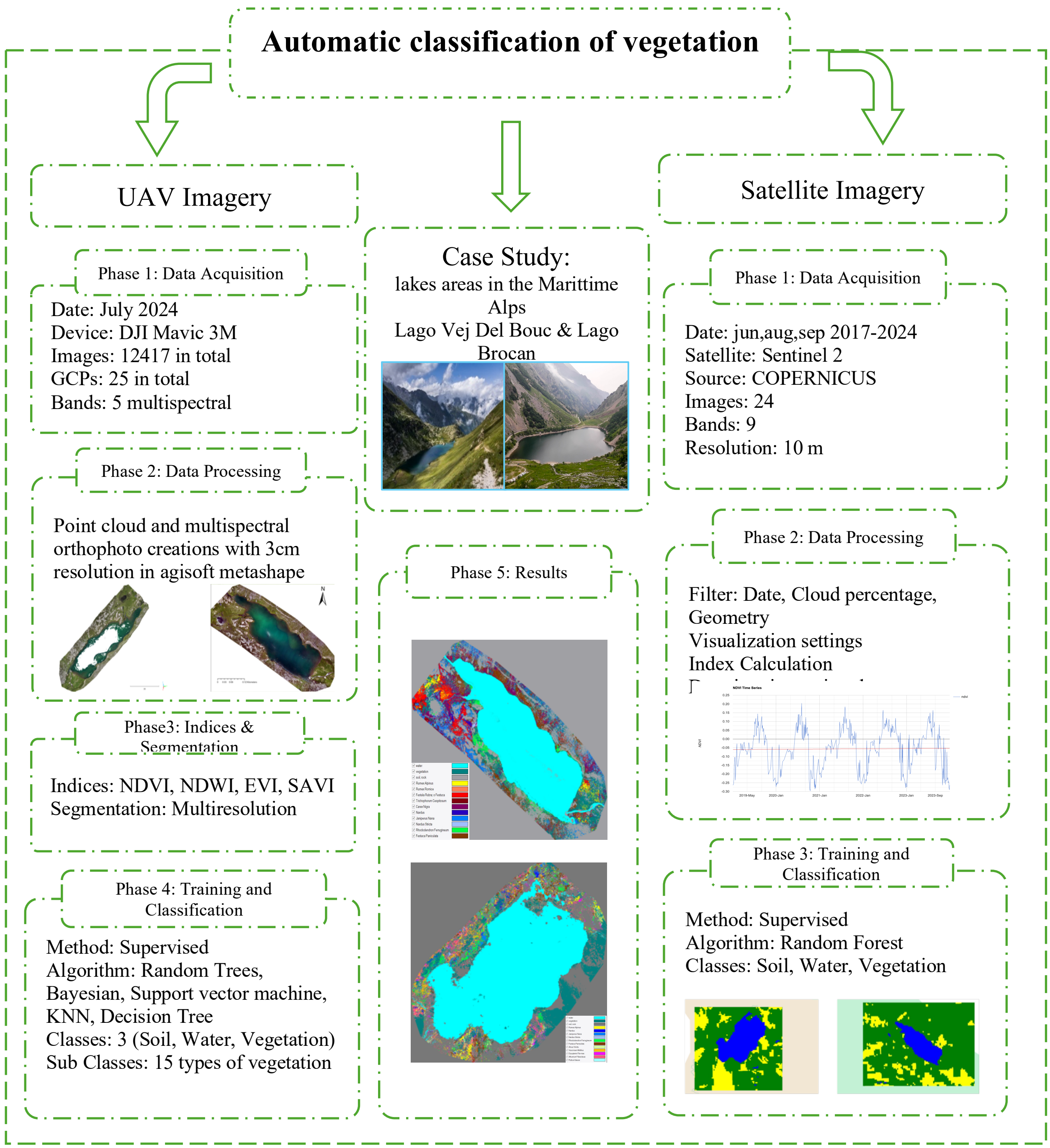

Figure 3-Methodology workflow

One advantage of this approach is the hybrid usage of object-based and pixel-based methods, which use both spatial and spectral knowledge in a balanced manner. The implementation of topographic corrections and seasonal imagery increased the accuracy of the classification. The utilization of UAV and Sentinel-2 data, in combination with an ensemble of machine-learning and deep-learning models, has proven to be a well-justified approach to cope with the difficulties of alpine vegetation mapping.

However, the scarcity of ground-truth data from the alpine study area could pose a challenge for the methodology. The rugged terrain and limited access to upland areas restricted the number of field samples that could be taken. To mitigate this, high-resolution UAV data were used as a guide for manual interpretation and labeling, and transfer learning was also used within deep learning to fully exploit the available labeled data across land-cover classes. Nevertheless, the methodological framework we developed in this research can be easily scaled and adjusted for other mountainous regions elsewhere.

3.1 Case Study: Lago Vej del Bouc and Lago Brocan, Maritime Alps

This case is based on Lago Vej del Bouc and Lago Brocan, two alpine lakes located in the Gesso Valley of the Maritime Alps (municipality of Entracque, Cuneo, Italy). They are excellent natural laboratories for studying the interrelationships of vegetation dynamics, hydrological variability, glacial dynamics, and human impacts in high-altitude catchments.

3.1.1 Geographical and Geological Context

Lago Brocan (2004 m a.s.l.) and Lago Vej del Bouc (2054 m a.s.l.) are situated in the Maritime Alps, whose rugged relief features steep ridges, glacially scoured depressions, and dramatic alpine scenery. These lakes were formed by ancient glaciers, and Lago Vej del Bouc in particular presents geomorphological evidence of glacial erosion that shaped the rock formations making up its basin. The region is also seismically and geomorphologically active, and strong local landslides and land-instability phenomena affect natural and human systems.

The lakes lie in the basins of the Vallone della Rovina and the Vallone del Vej del Bouc, each of which drains into the larger watershed of the Torrente Gesso, a high-altitude Alpine system.

3.1.1.1 Climate and Hydrology

This area enjoys a moderate alpine climate with warm, active growing-season summers (June–August) and increased precipitation in September, influencing vegetation cycles and lake hydrodynamics. The lakes are mainly sustained by glacial melt and seasonal precipitation, so seasonal changes and short-term water-level fluctuations are the norm. This hydrologic pattern is essential for maintaining local biodiversity but is also highly susceptible to ongoing climate change.

Lago Brocan is part of a pumped-storage hydropower system managed by ENEL and, along with the Chiotas Dam, forms the reservoir feeding water to the Centrale Idroelettrica Luigi Einaudi, one of Italy's most important hydroelectric plants. This artificial regulation modifies natural hydrological cycles, offering a remarkable natural experiment for investigating the impacts of pumped-storage plants on alpine lake ecosystems.

3.1.1.2 Vegetation and Ecological Characteristics

The vegetation of both lake basins is highly heterogeneous, comprising natural grasslands, mixed deciduous–conifer forests, and shrublands that differ in species abundance according to altitude, soil type, and available soil moisture. These plant assemblages are excellent indicators of environmental change and provide valuable information on alpine ecological mechanisms under climatic and anthropogenic stress.

3.1.1.3 Accessibility and Cultural Significance

Although remote, both lakes can be reached via cairned alpine trails. Lago Vej del Bouc can be accessed from San Giacomo di Entracque (1209 m) with a 1–2 h walk that passes through habitats ranging from beech stands to high-alpine pastures. Lago Brocan can be approached from Lago della Rovina, but the route is more challenging and includes waypoints at Rifugio Genova Figari and the Chiotas Dam. Both lakes form part of a wider alpine trekking network, although the continuity of routes has been interrupted by landslides and flood events, especially in 2008/09 and 2013/14, highlighting the terrain's precariousness.

In terms of cultural significance, Lago Vej del Bouc is known for its prehistoric rock art dating to the second millennium BC. These carvings bear witness to early human presence and interaction with the alpine landscape, making the site important for historical and archaeological studies.

3.1.1.4 Human Impact and Hydropower Development

Lago Brocan is an important reservoir within a regional hydroelectric scheme that includes the lower Chiotas Dam. This system generates renewable energy but also causes hydrological changes that affect water quality, aquatic biodiversity, and ecosystem services.

The abandonment of a dam-submerged building in the 1970s, later replaced by Rifugio Genova Figari, exemplifies the ongoing balance between environmental concerns and economic interests. The region is a microcosm illustrating the challenge of managing alpine ecosystems amid intense energy demand and conservation goals.

3.1.1.5 Environmental Challenges and Future Directions

Both lakes face increasing environmental stressors such as glacial retreat linked to climate change, greater hydrological variability, and hazards like landslides and floods. Trail erosion and the loss of infrastructure (e.g., the footbridge to the POLARIS research area in the Vej del Bouc valley) demonstrate measurable impacts on ecological research and sustainable tourism.

Seasonal water-level regulation for hydropower raises questions about the sustainability of energy use in vulnerable habitats. Long-term studies are needed to track human impacts on the lakes, associated pollution, and the sensitivity of indigenous species under changing conditions.
The Lago Vej del Bouc and Lago Brocan case study demonstrates the intricate relationships among natural processes, ecological systems, and human activities in the Maritime Alps. Beyond their roles as ecological and hydrological indicators, the lakes are also valuable cultural and historical assets. Integrating environmental monitoring, sustainable energy management, and cultural-heritage preservation is vital for the long-term health and stability of this unique alpine environment.

3.2 Dataset

To obtain a full picture of vegetation and water dynamics in the area, both satellite and drone-based RS images have been applied in this study. Combining the multi-resolution datasets enabled detailed temporal and spatial investigations over seasons and years. Medium-resolution multispectral Sentinel-2 satellite imagery was used for long-term trend analysis, and high-resolution drone imagery for local-level validation and precision mapping. The two datasets were pre-processed and analyzed to derive spectral indices and classify the land cover. The specifications and properties of the data are described in the next sections.

3.2.1 Satellite Imagery

Satellite data for the study area were obtained from Sentinel-2 MSI (Multispectral Instrument), which offers medium-resolution imagery favorable for environmental monitoring. Twenty-four multispectral images were chosen to represent the period from June 2017 to September 2023 and support multi-annual monitoring of vegetation and water-body trends. The following photo showing a sentinel-2 image in sentinel-hub.com, on 16 June of 2017 with cloud cover of 8.5 percent.

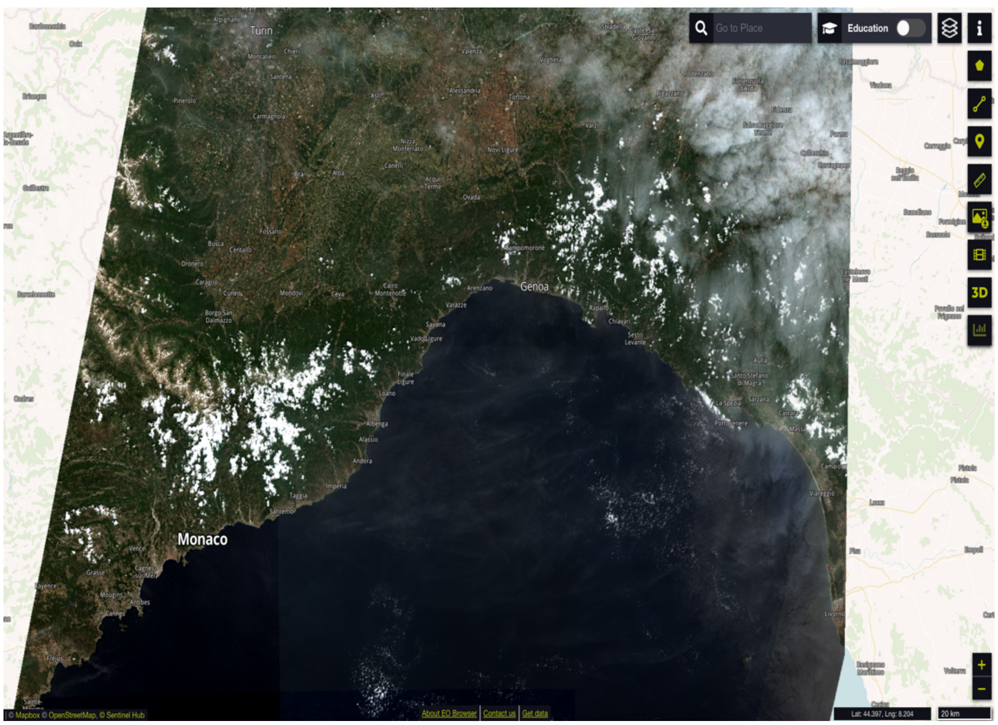

Figure 4-sentinel-2 image sample

The satellite data consist of four key spectral bands: band 2 (blue), band 3 (green), band 4 (red), and band 8 (near-infrared), which are widely employed in vegetation and water analyses because of their spectral sensitivity. From these band combinations we calculated several spectral indices, such as the Normalized Difference Vegetation Index (NDVI), the Normalized Difference Water Index (NDWI), and the Soil-Adjusted Vegetation Index (SAVI), to more accurately describe vegetation condition and water distribution in the study area.

The images have a 10 m resolution, providing a balance between detail and regional coverage. Images were obtained on a monthly basis, with a focus on the months of June, August, and

September in the respective years, in order to record seasonal variation in vegetation cover and water levels. The region of interest covers the surroundings of Lago Vej del Bouc and Lago Brocan, guaranteeing complete spatial coverage of the alpine ecosystems studied in this work.

3.2.2 UAV Imagery

As part of the wider investigation within the ACLIMO project, two high-altitude alpine lakes, Lago Brocan and Lago Vej del Bouc, were mapped in July 2024 using photogrammetric UAV techniques. Those surveys were performed with a DJI Mavic 3M drone equipped with a Real-Time Kinematic (RTK) positioning module to guarantee high spatial accuracy. These operations aimed to acquire ultra-high resolution orthophotos for vegetation classification and to support broader environmental monitoring (lake morphology, terrain and vegetation structure, ecological changes). The rout of the flight and location of camera in both lakes are shown in the figure 4.

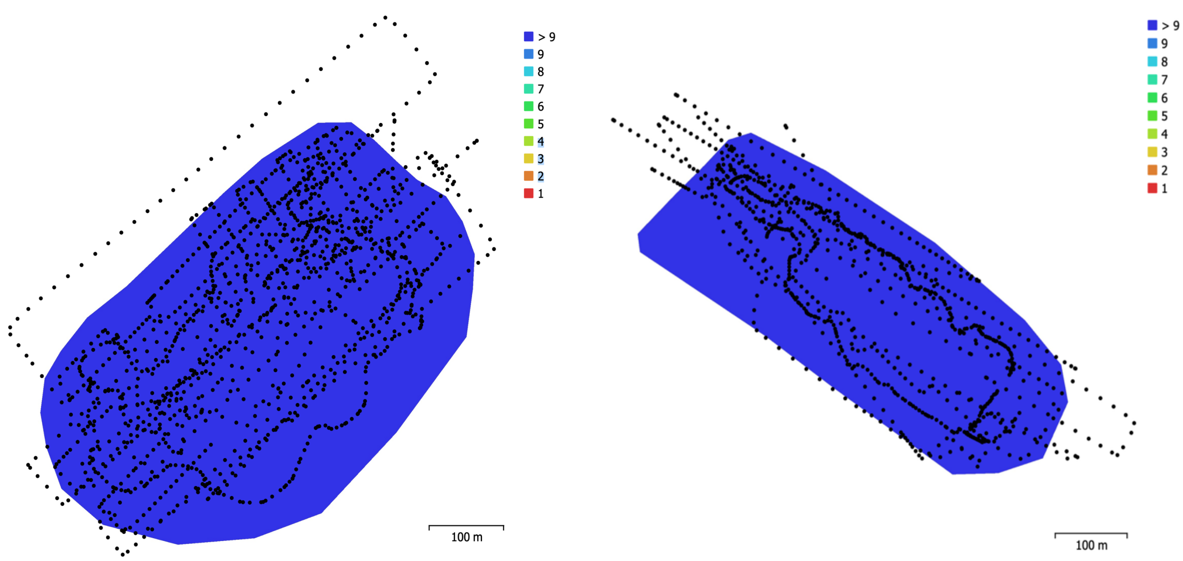

Figure 5-Flight rout in both lakes

For the UAV campaigns, 4 947 images were acquired over Vej del Bouc and 7470 images over Brocan. The flights were designed for maximum overlap and consistent illumination to avoid inclination effects caused by shadows or relief. Ground control points (GCPs) were distributed at both sites, 7 at Vej del Bouc and 18 at Brocan, to georeferenced the image sets and calibrate the reconstructed 3-D model photogrammetrically. Initial processing in DJI Terra produced dense point clouds of approximately 28.1 million and 32.5 million points for Vej del Bouc and Brocan, respectively, with expected root-mean-square errors (RMSE) of 2- 3 cm.

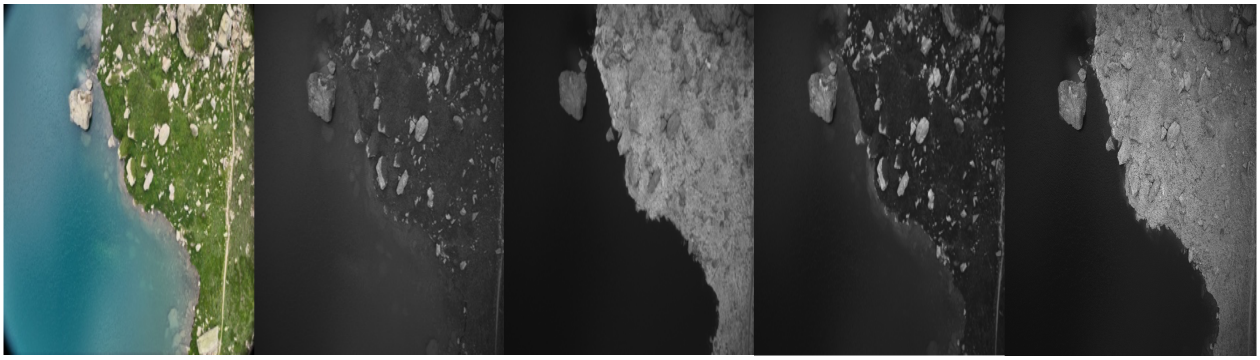

Figure 6-Example of a multispectural image with 5 bands (RGB, Green, NIR, Red, Red Edge)

Despite adequate point density, co-registration accuracy and spectral consistency were compromised, especially between multispectral bands. To remedy this, all imagery was reprocessed in Agisoft Metashape Professional, allowing more reliable alignment and control of photogrammetric parameters. Two workflow methods were evaluated. Initially, bands were resampled into a single file, but this produced small mis-registration residuals and poor correspondence between spectral layers. Consequently, a more conservative approach was adopted: each spectral band (RGB, Red, Green, Red-Edge, and NIR) was processed as an independent chunk per lake. This band-separation strategy generated five high-resolution orthophotos for each lake, achieving sub-decimeter resolution and co-registration accuracy better than 3 cm. The following screenshots illustrating the steps of image processing in Agisoft Metashape, including importing images in 5 different chunks and aligning the images and creating the tie point (Fig. 7).

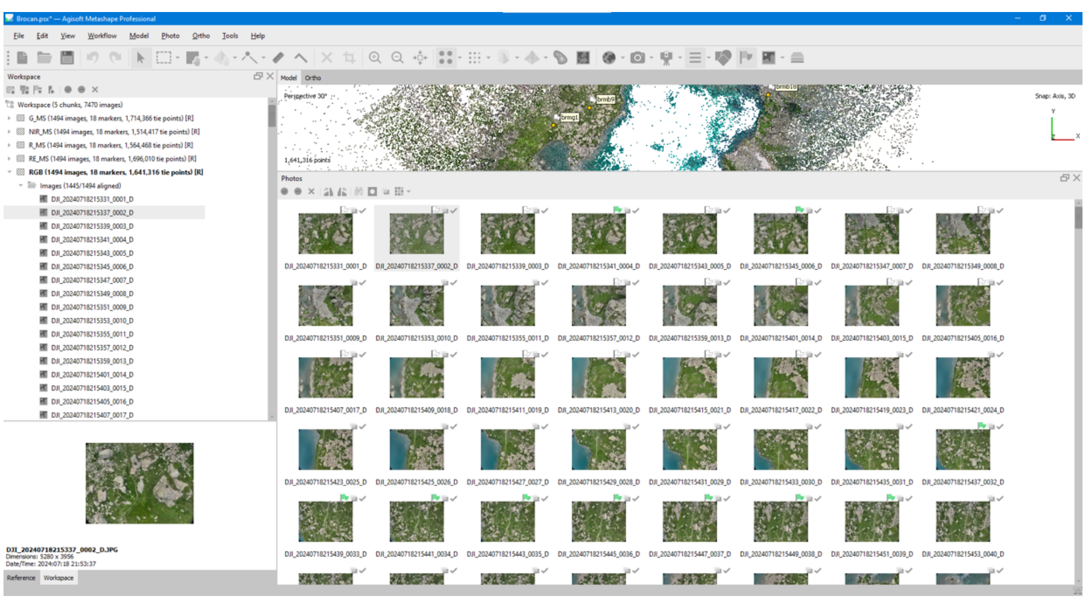

Figure 7-Importing and ilignment of images and creating tie point

Ground Control Points (GCPs) were imported into Metashape and manually marked by placing each marker precisely at the center of its corresponding target across multiple image frames. This manual marking ensured accurate georeferencing and formed the basis for subsequent alignment optimization and bundle adjustment. (Fig. 8)

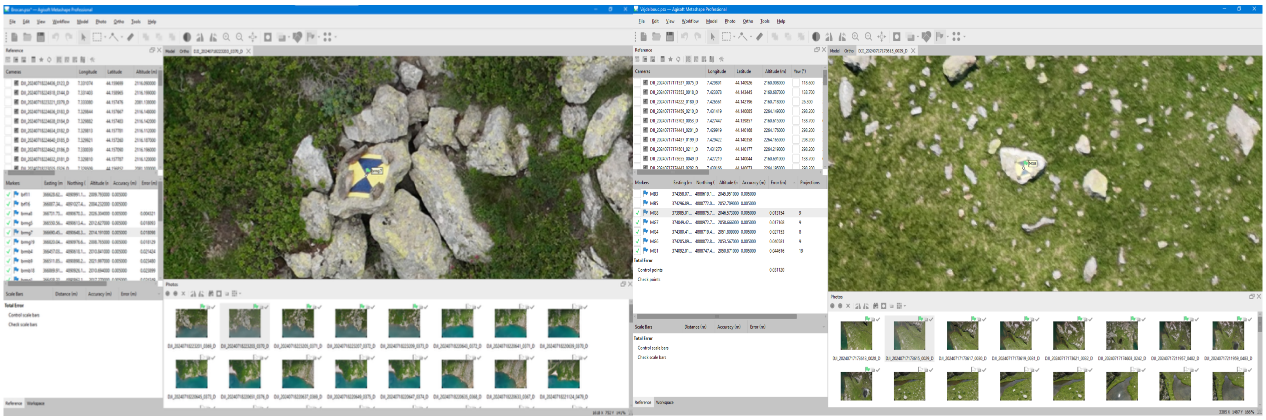

Figure 8-Importing and Georeferencing GCPs for both lakes

Following marker placement, the model underwent optimization through bundle adjustment, significantly improving the spatial accuracy of the photogrammetric outputs. The total root mean square (RMS) error for control points was 0.028 m for the Brocan dataset and 0.031 m for the Vej del Bouc dataset, indicating high georeferencing accuracy. The number of projections per marker varied based on visibility across image sets, with some markers exceeding 15 projections, further reinforcing the geometric reliability of the reconstructed models. (Fig. 9)

Markers	Easting (m	Northing (	Altitude (n	Accuracy (m)	Error (m)	Projectio
brf11	366628.62...	4890991.1...	2009.793000	0.005000		0
brf16	366887.34...	4891027.4...	2004.232000	0.005000		0
brma8	366731.73...	4890670.3...	2026.304000	0.005000	0.004321	3
brmg5	366550.56...	4890613.4...	2012.627000	0.005000	0.018093	8
brmg7	366690.45...	4890648.3...	2014.191000	0.005000	0.018098	5
brmg19	366820.04...	4890976.6...	2008.765000	0.005000	0.018129	16
brmb4	366457.03...	4890618.1...	2010.841000	0.005000	0.021424	8
brmb9	366511.85...	4890898.2...	2021.997000	0.005000	0.023480	15
brmb18	366869.91...	4890926.1...	2010.694000	0.005000	0.023899	14
brmg1	366438.32...	4890863.1...	2017.270000	0.005000	0.024349	6
brmb6	366634.35...	4890613.8...	2011.022000	0.005000	0.025179	5
brmg15	366813.09...	4891050.3...	2008.143000	0.005000	0.027264	11
brmg13	366737.43...	4891078.1...	2008.244000	0.005000	0.028484	12
brmb14	366792.79...	4891109.6...	2011.496000	0.005000	0.029742	6
brmg17	366866.14...	4890992.4...	2010.808000	0.005000	0.035206	6
brma2	366375.62...	4890743.9...	2013.193000	0.005000	0.037312	9
brmb12	366651.64...	4891005.0...	2007.733000	0.005000	0.041696	17
brmg3	366387.80...	4890664.6...	2010.579000	0.005000	0.043981	14
Total Error						
Control points					0.028012	

Markers	Easting (m	Northing (	Altitude (n	Accuracy (m)	Error (m)	Projections
MB3	374358.07...	4888619.1...	2045.951000	0.005000		
MB5	374296.89...	4888772.0...	2052.709000	0.005000		
MG8	373985.01...	4888875.7...	2046.573000	0.005000	0.013154	9
MG7	374049.42...	4888972.7...	2058.666000	0.005000	0.017168	9
MG4	374380.41...	4888719.4...	2051.809000	0.005000	0.027153	8
MG6	374205.89...	4888872.8...	2053.567000	0.005000	0.040581	9
MG1	374092.01...	4888747.4...	2050.871000	0.005000	0.044616	19
Total Error						
Control points					0.031120	
Check points						

Figure 9-RMSE for each point and total error under 4 CM

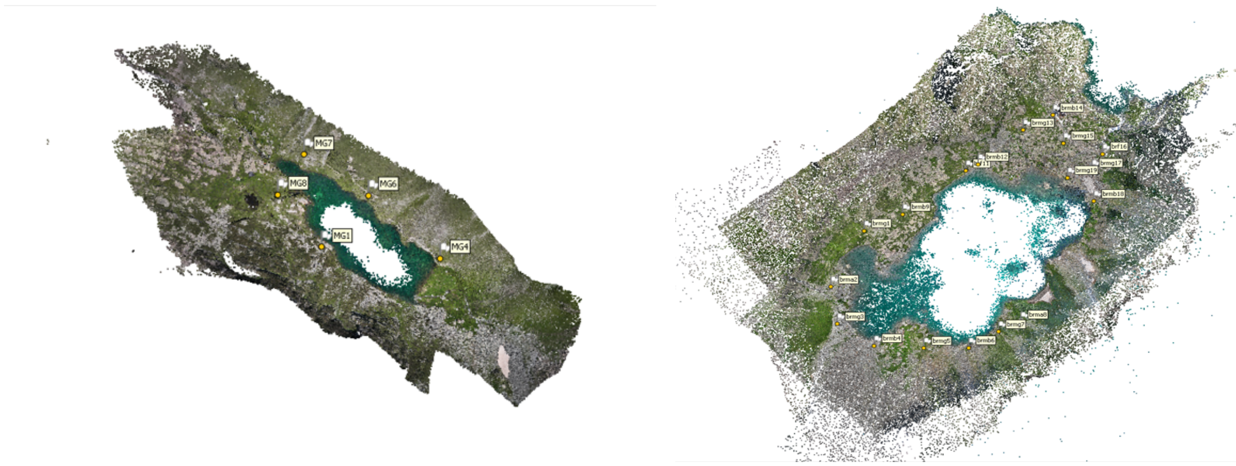

Figure 10-Position of GCPs around the lakes

The resulting orthomosaics served as the base for a two-stage vegetation-classification workflow in eCognition Developer. In the first stage, object-oriented classification detected the main landcover classes. Segmentation was performed with multiresolution algorithms, after which spectral, spatial, and textural features were extracted. In all cases, five classifiers (Bayesian, SVM, KNN, Decision Tree, and Random Forest) were tested and compared in this initial classification.

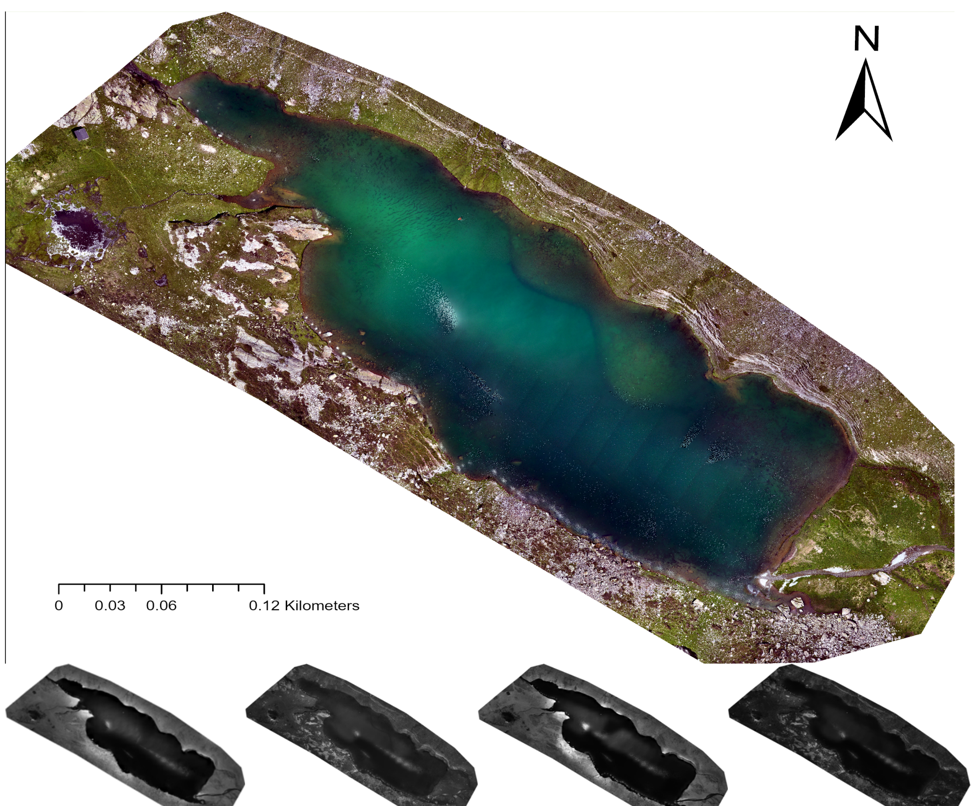

Figure 11-Vej Del Bouc Lake final RGB and multispectral orthophotos

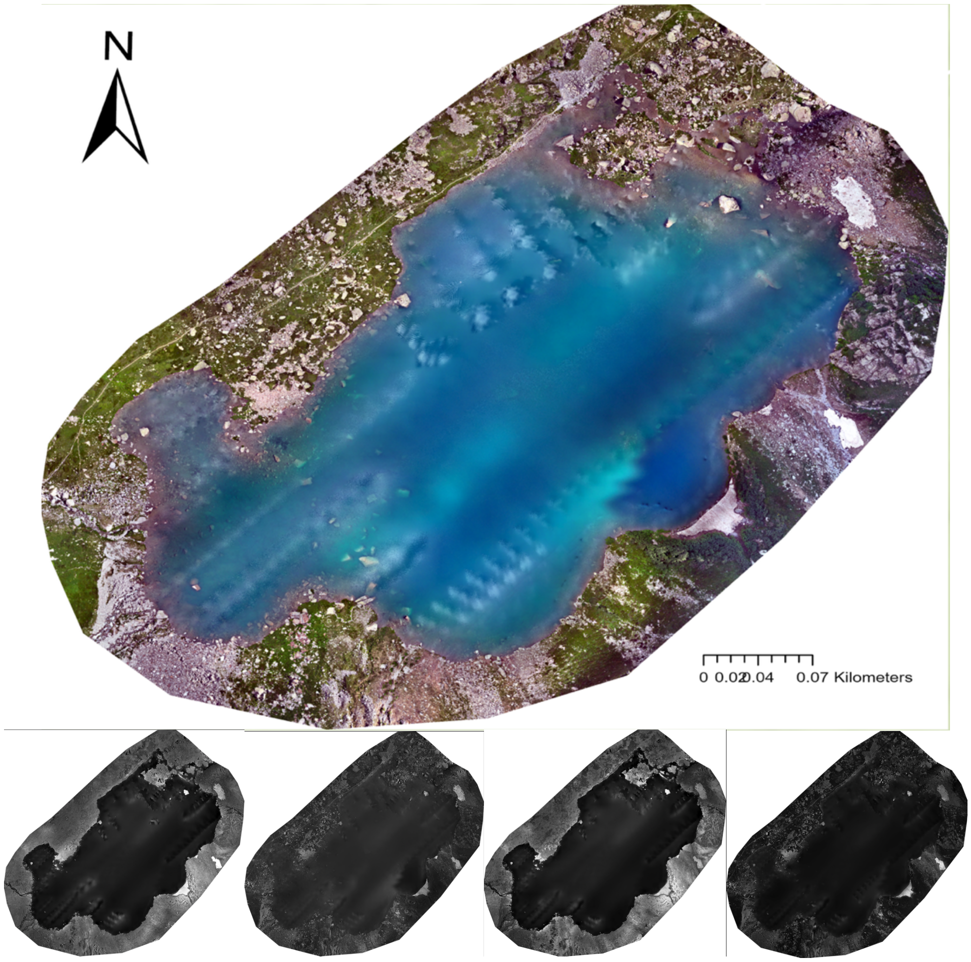

Figure 12-Brocan Lake final RGB and multispectral orthophotos

In the second stage, analysis focused on vegetated areas. A refined vegetation-type classification was carried out using ground-truth data collected during the 2024 UAV field campaigns. These samples trained and validated separation between the dominant vegetation types surrounding the two lakes. Following the previous OBIA method, all five machine-learning algorithms were again executed in parallel to evaluate their performance in differentiating vegetation classes. This hierarchical approach enabled high-resolution, ecologically relevant classification.

The UAV-based component of this study delivered high spatial accuracy, rich multispectral information, and strong methodological adaptability. Its integration within the ACLIMO project demonstrates a scalable and robust model for alpine ecosystem monitoring, vegetation classification, and geomorphological analysis in high-altitude environments.

3.3 Data Processing

The workflow followed here focused on obtaining accurate and informative outputs from both UAV and satellite imagery, facilitating a multiscale assessment of vegetation and hydrological dynamics in the Lago Vej del Bouc and Lago Brocan regions. Raw data from these sources were systematically preprocessed, corrected, and analyzed to provide consistent-quality data in time and space. Sentinel-2 multispectral image data were acquired and processed in GEE, a helpful cloud-based platform for filtering, clipping, correcting, and analyzing large amounts of data. Selected vegetation and water indices were derived to follow up seasonal variations and to classify land-cover modalities.

Simultaneously, high-resolution RGB drone imagery acquired during field operations was processed through photogrammetric software to create orthophotos and Digital Surface Models (DSMs). This fine-scale dataset provided location-specific ground details for validating satellite-based land-cover classification and detecting fine-scale land-cover changes. Emphasis was placed on making the datasets spatially and temporally congruent, thereby minimising potential offsets caused by temporal cloud cover, topographic shadow, or sensor misalignment.

The following sections provide a detailed breakdown of the processing steps specific to each data type:

3.3.1 Satellite Imagery

The satellite-based part of this study was used as a coarse-resolution tool to monitor long-term changes in vegetation and water conditions over the two alpine lakes, Lago Vej del Bouc and Lago Brocan, under the larger ACLIMO project. This assessment offered a multiple-year window on vegetation to coincide with the more detailed UAV classification and provided necessary seasonal and interannual environmental context.

Satellite imageries were obtained from the Sentinel-2 Multispectral Instrument (MSI) data which can be downloaded from the Copernicus Open Access Hub. Both Level-1C (top-of-atmosphere reflectance) and Level-2A (atmospherically corrected surface reflectance) were explored, from which data was chosen based on availability and processing requirements. To avoid data with poor quality, the scenes with cloud cover over the study area exceeding 10% were not used. All images were visually checked to verify whether the lakes and surrounding vegetated areas were fully visible.

The time frame of the study spanned 2017–2024, emphasizing three important seasonal periods: June, August, and September. We selected these months based on the optimal period of time to capture the main components of alpine vegetation growth and waterbodies dynamics (June, during snowmelt peak and early vegetation growth; August, when canopy development cycle had been completed and lake levels were stable; and September, late vegetation senescence, potential first returning signal of new snow). The choice is consistent with climate and vegetation gradients detected by ARPA Piemonte and other alpine ecological reference frameworks.

All pre-processing and analyzing were conducted in Google Earth Engine (GEE), a cloud-based computing platform optimized for creating large-scale remote sensing workflows. The Sentinel-2 collections were filtereded by date, cloud cover, clipped spatially to the exact AOI extents, and quality was restored based on the QA60 band for cloud masking. For Level-1C products, atmospheric correction tasks in GEE were performed to normalize reflectance values and to cancel out atmospheric noise.

Following pre-processing, each of the images was resampled to an RGB composite and analyzed for four important spectral indices that yield complementary information on surface conditions and ecological processes: NDVI, NDWI, EVI, and SAVI.

The NDVI, the established parameter for vegetation health and productivity, was the main parameter used to evaluate the condition of vegetation during the investigation. It facilitated monitoring of greenness and interannual variations, especially the range in high altitude meadows and forested slopes. The Normalized Difference Water Index (NDWI) was employed to map shallow water bodies in the monitoring of conditions around the edge of lakes during the summer melt and dried period.

The Enhanced Vegetation Index (EVI) was computed to improve value in high vegetated areas. The addition of the blue band enhanced atmospheric correction and reduced the background noise and was useful for mapping structural vegetation changes in areas with a full canopy cover. Meanwhile, the Soil-Adjusted Vegetation Index was used in sparsely vegetated rocky areas, where contribution from soil-reflectance might be masking weak signals from vegetation – this was valuable on rocky alpine faces with patchy plant cover.

For each of the four indices we produced maps for the individual lakes in all three target months for all years from 2017 to 2024. These spatial predictions were further complemented with temporal trend analysis. Average index values for each lake, month were then calculated, and these data plotted as multi-year line charts to allow qualitative assessment of an oscillating ecological signal and longer-term ecological direction. These maps contributed to the interpretation of the changes observed in vegetation cover and water levels and provided a global vision of both at different time and space scales.

Land cover mapping was performed only with Random Forest (RF) in the Google Earth Engine (GEE) cloud computing platform. The criteria for this selection were the efficiency of the method in high-dimensional feature spaces and the robustness of the approach against overfitting. The training samples were manually digitized with reference to the UAV orthophotos and visual interpretation of Sentinel-2 scenes. Four major land cover types were classified, including open water, bare soil or rock, sparse, and dense vegetation.

The RF classifier was trained based on Sentinel-2 spectral bands and calculated indices as input features. The model was then applied in all the chosen scenes to produce consistent land cover maps at a 10-m interval. Classification products were exported from GEE as GeoTIFF and analyzed in GIS (e.g., ESRI ArcGIS, QGIS), for comparison and validation compared to UAV-derived outputs.

In summary, the satellite imagery analysis generated a data set that is both robust and scalable as well as temporally richer and improved the vegetation and water dynamics data set for the study alpine catchment, adding to the integration of local-scale UAV-based surveys and the broader remote sensing context. Such two-step workflow helps long-term ecosystem monitoring, landscape-level change detection, and climate impact evaluation in complex mountainous landscapes.

3.3.2 UAV Imagery

Data processing carried out from UAV was the key to the present manuscript, as it delivered the ultra-high-resolution geospatial information necessary for a vegetation classification and topographic analysis of the study sites (Lago Vej del Bouc and Lago Brocan). These drone surveys were performed with a DJI Mavic 3M equipped with an RTK module, driven by the ACLIMO project in July and October 2024, allowing for centimeter-level geolocation precision. In the case of Lago Vej del Bouc, 4,947 images were acquired and 6,116 for Lago Brocan, with scheduled overlaps that allowed optimal co-registration and 3D reconstruction. In the survey areas, ground control points (GCPs) (seven for Vej del Bouc and ten for Brocan) were established and measured using GNSS in order to provide a reliable geospatial reference for the image processing analysis.

The raw images were post-processed in DJI Terra, with its High Precision 3D Reconstruction workflow. This first stage also involved automatic camera calibration, feature-matched image registration, and bundle adjustment. Multi-view stereo algorithms in the software then produced sparse and dense point clouds, and the model had 28.1 million and 32.5 million 3D points for Vej del Bouc and Brocan, respectively. However, spectral offsets were observed, and the spatial coherence required for multispectral assessment was not satisfactory, where a more robust and flexible workflow was adopted in Agisoft Metashape Professional, although a total error of 2 to 3 cm was still evident.

For each spectral band, we performed the photogrammetric processing at high resolution in Metashape. The steps start from registration and calibration of the camera to feature-based tie-point generation and optimization on the automatically derived key points with reference to the GCPs that are marked manually. Spatial referencing was improved using bundle adjustment, and residuals of GCPs were checked to ensure position accuracy of 2–3 cm. After registration, point clouds were computed and thus depth maps were obtained that contained information of the 3D surface structure of the landscape. (Figure 3)

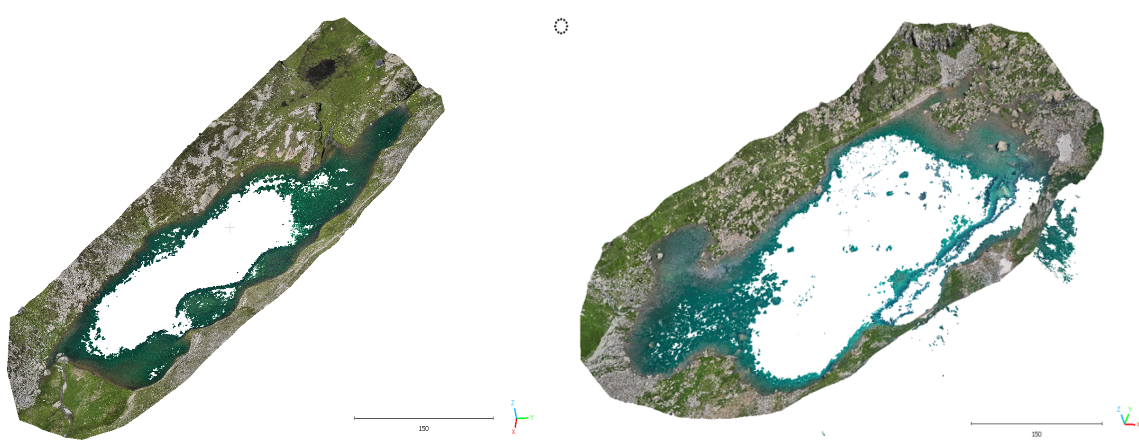

Figure 13-Point clouds created in Agisoft metashape

Orthophoto production was carried out independently for each of the five spectral bands (RGB, Red, Green, RedEdge, and NIR) because when we initially tried processing all bands in a single chunk, due to co-registration, the process failed. This band-separation approach facilitated clean orthorectification whereby the spectral information is not lost. The resulting orthophotos, at a resolution nearing 3 cm/pixel, were assessed with GCP residue reports and visual map comparisons with satellite basemaps. In the figure 14 the correction of co-registration error is shown.

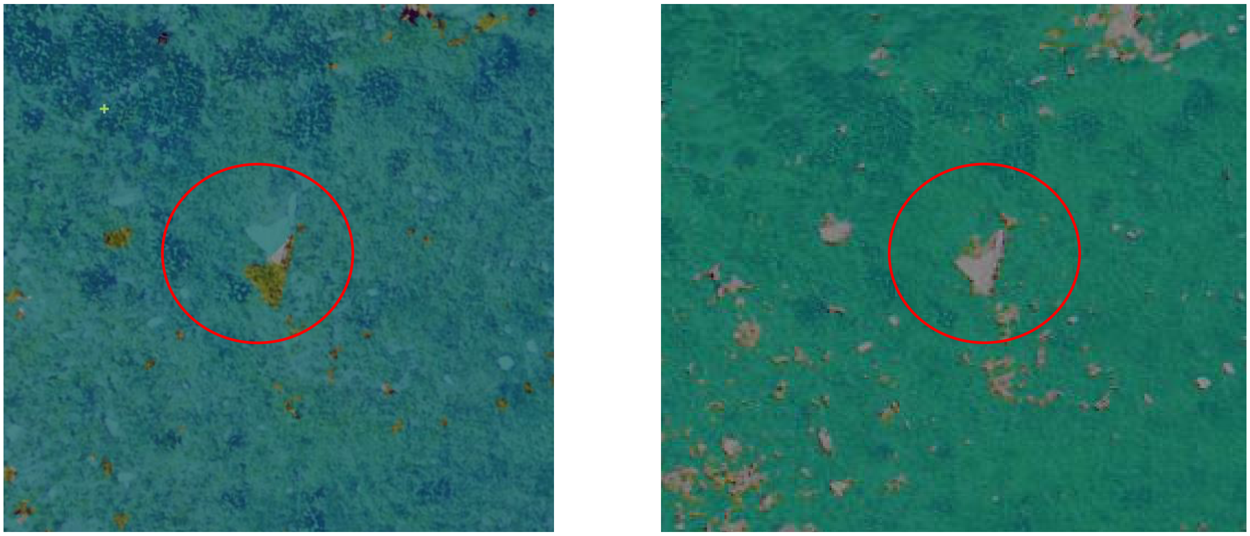

Figure 14- Co-registration error fixed

DSMs were also calculated from the dense clouds to represent changes in elevation of both vegetated and non-vegetated surfaces. Though radiometric errors and inconsistencies were induced due to the mountainous topography and temporal variability in the scene illumination/shadows, these were resolved via careful masking and processing parameter values.

The results of this phase, what Balice et al. Magnetometry (2008) refer to as band-specific orthophotos and DSMs, provided the basis for classification in eCognition and also supplied an accurate spatial dataset for characterizing alpine vegetation patterns.

3.3.3 Object-Based Classification

Land cover and vegetation categorization was conducted in eCognition Developer, through the object-based image analysis (OBIA) workflow. For each spectral band (RGB, Red, Green, RedEdge, NIR), orthophotos generated using Agisoft Metashape were imported into eCognition as separate image layers. This framework achieved complete spectral agility and was suitable for multi-band object-level feature extraction.

In order to increase the discriminative power of the classification, a series of spectral indices were calculated directly in eCognition with the help of the process tree. These were NDVI, NDWI which were formulated from the respective custom bands with formula nodes. First, classification was attempted using multi-threshold segmentation with the defined index thresholds to distinguish water, soil/rock, and vegetation. However, this method had low classification accuracy, with visible edge artefacts in shadow and transition areas.

A more complex segmentation approach was therefore applied: multiresolution segmentation (based on scale, shape, and compactness parameters) to cluster grouped pixels as homogeneous objects. Crucially, the representation parameters, defined as the custom weighted values for each band, could be tuned, with the power of NIR and RedEdge for discriminating vegetation combined with the strength of Green and Blue in distinguishing water and soil.

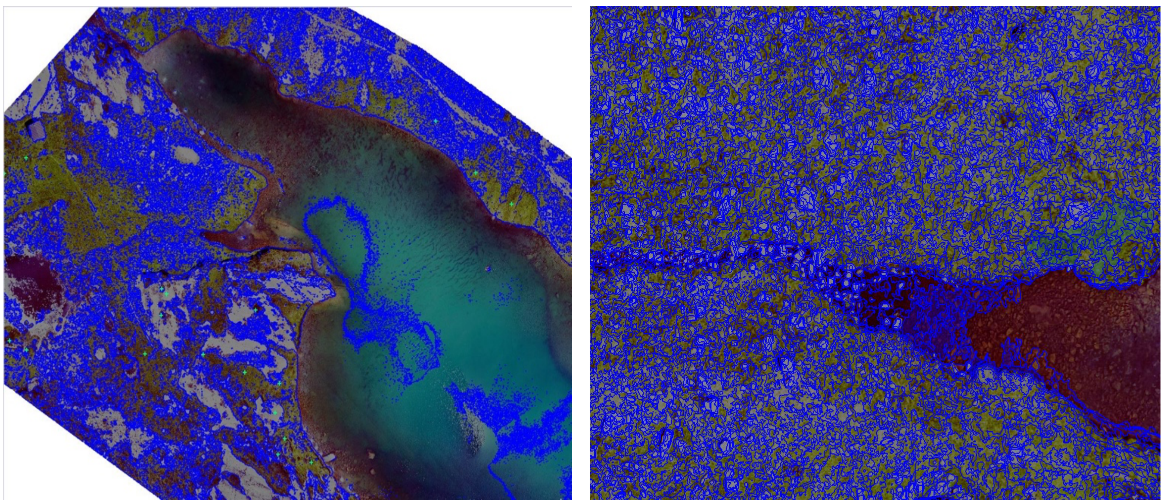

Figure 15-multi threshold segmentation(left), vs multi resolution segmentation(right)

After obtaining the optimal segmentation, a large training set was created for the supervised classification. In total, twenty thousand examples for water, seventeen thousand for soil/rock, and eighteen thousand for vegetation were labelled and employed for training the classifiers. These samples spanned spectral variability across the lakes and in the surrounding terrain, which experienced shadow, variable vegetation coverage, and mixed pixels.

The first grouping phase was set to differentiate between the broad land-cover types of water, soil/rock, and vegetation. These samples were then subjected to five supervised machine-learning algorithms in eCognition: Bayesian, SVM, KNN, Random Tree, and Random Forest. Each classifier was trained separately and operated independently, and classification performance was evaluated by matching outputs to known object classes and through visual validation.

After the overall land-cover classification, a second classification step was implemented to obtain vegetation types. Field studies on the shores of both lakes (both lakes were covered by UAV campaigns) served to ground-truth samples of the dominant plant species and vegetation communities. These samples were used to determine the training set for vegetation sub-classes. The enhanced dataset was used to repeat the five classifiers to assess their performance in fine-scale ecological classification. This two-tiered categorization can produce both general land-cover maps and more specific ecological interpretations of the vegetated landscape in the alpine-lake areas.

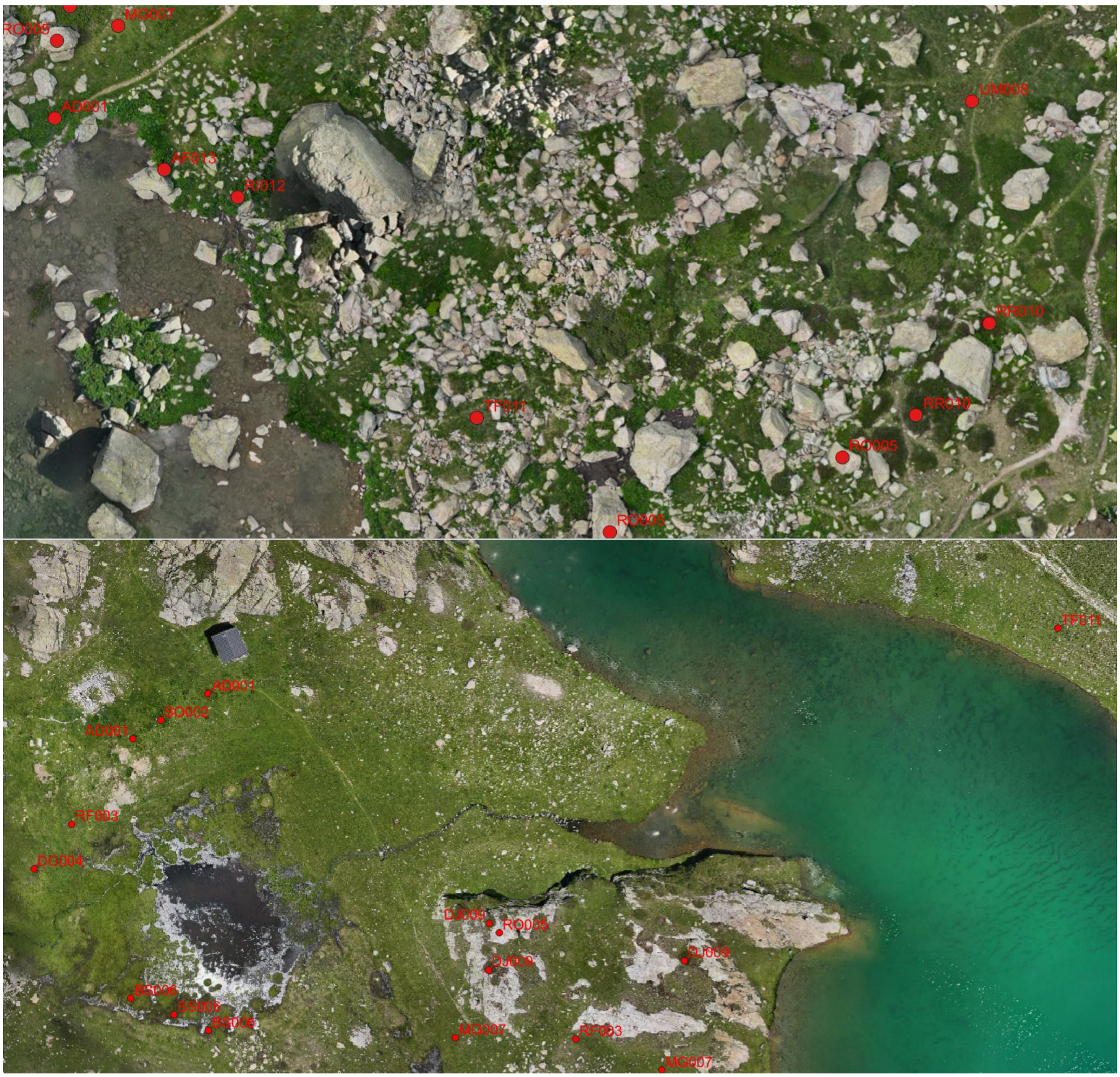

Figure 16-Position of vegetation samples in both lakes

Table 3-Vegetation types and codes

	Italian Name	English Name	Code
1	Rumex Alpinus	Alpine Dock	AD001
2	Rumex Romice	Sorrel	SO002
3	Festula Rubra; o Festuca	Red Fescue	RF003
4	Trichophorum cespitosum	Deergrass	DG004
5	Carex nigra	Black Sedge	BS006
6	Nardus	Matgrass	MG007
7	Nardus Stricta	Upright Matgrass	UM008
8	Janiperus nana	Dwarf Juniper	DJ009
9	Rhododendron Ferrugineum	Rusty-Leaf Rhododendron	RR010
10	Festuca Paniculata	Tussock Fescue	TF011
11	Rubus Idaeus	Red Raspberry	RI012
12	Athurrium Filixoideas	Lady Fern	AF013
13	Dryopteris Flix-max	Male Fern	DF014
14	Vaccinium Mirtillus	Bilberry	VM015
15	Alnus Viridis	Green Alder	AV016

In combination, inclusion of multi-band orthophotos, spectral-index layers, optimized segmentation, and supervised machine learning in eCognition yielded a solid and repeatable procedure for object-based classification. This part of the thesis was necessary to convert the raw UAV data into relevant ecological information, which is highly valuable for future monitoring in comparable alpine systems.

4 Results

The results of the analyses conducted using Google Earth Engine (GEE), DJI Terra, Agisoft Metashape, and eCognition are presented in this section for both satellite and UAV imagery. The combined multi-temporal and multi-scale data allowed a dense and multilayered view of vegetation and water body dynamics within the study region. Satellite acquisition facilitated multiscale temporal and land cover trend analysis, whereas UAV-derived imagery provided spatially detailed, fine-scale information needed for classifying vegetation and validating medium-resolution products.

4.1 Satellite Imagery

Sentinel-2 imagery arranged in GEE code was used to evaluate land cover dynamics of the study area over the period between 2017 and 2024. The dataset was sensitive in summer (i.e., June, August, and September), when the activity of vegetation and hydrological dynamics reached the maximum.

Composite RGB images were created for each year and lake, and the four most important spectral indices, NDVI, NDWI, EVI, and SAVI, were calculated. Index values were visualized in annual index maps and means were calculated per lake and season. The resulting series of datasets were shown in multiannual time series graphs (Fig. 17), to illustrate patterns of vegetation condition, water stress, and soil–vegetation dynamics. NDVI values were uniformly high in August, reflecting maximum vegetation health, and dropped in September. In contrast, NDWI values presented interannual variability associated with precipitation and ice melt lake input, and lake surface decreased during drier years.

Figure 17-NDVI annual timeseries

For each selected scene, a Random Forest classifier was trained using a mixture of spectral bands and index layers. Three land cover classes were detected by the classifier: open water, vegetation, bare soil/rock. The classification results (GeoTIFFs) were exported and visually checked using UAV-based orthophotos.

Classification maps were validated by reference data based on the UAV images. The Random Forest model provided classification accuracies of 85 to 92%, depending on the year and cloudiness.

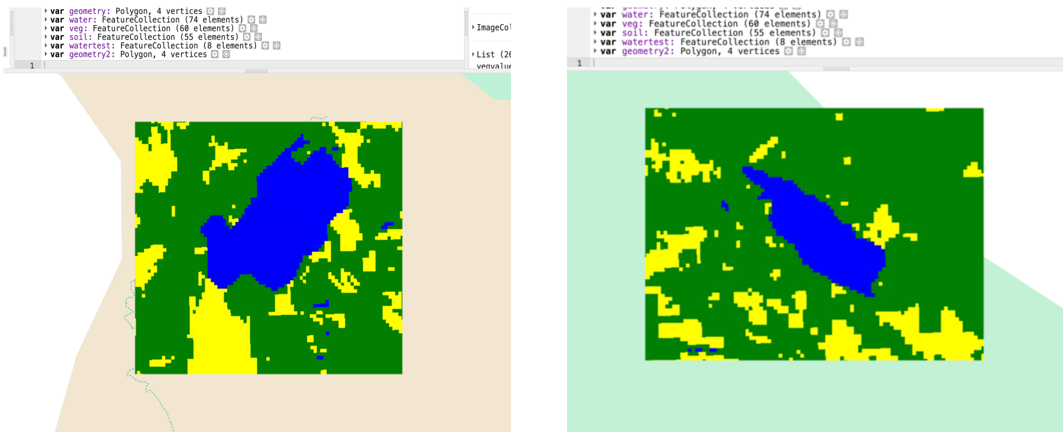

Figure 18-Random gorest classification in GEE

The post-classification change detection indicated that there has been a gradual reduction in the extent of dense vegetation cover, particularly at the edges of those on upper slopes. Reduced lake extents were seen in the most arid years (e.g., 2022) and were combined with declines of the NDWI. Vegetation belts seemed to rise, most likely in response to glacial retreat and the warmer climate developing (Fig. 18).

4.2 UAV Imagery

UAV multispectral imagery, processed in Agisoft Metashape and classified using eCognition, produced ultra-high-resolution outputs with decimetric positional accuracy. Following image capture using DJI Mavic 3M, the ortho-images and digital surface models (DSMs) were created using photogrammetric procedures that involved camera calibration, point cloud production, and orthorectification. Accuracy of the input material was ensured by processing each spectral band individually in ortho-photo production. The ortho-photos were then used as input for OBIA.

The classification procedure in eCognition started with band-separated orthophotos followed by multiresolution segmentation. The vegetation indices (NDVI, NDWI) were also calculated in a single module (process tree), and an initial multi-threshold segmentation was tried using index values. As the accuracy was not acceptable, the workflow was altered towards multi-resolution segmentation with customized weights per spectral band, resulting in a much-increased segmentation accuracy.

A supervised classification was applied using training samples from objects that were segmented out. To train five classifiers—Bayesian, SVM, KNN, Decision Tree, and Random Forest—20,000 water segments, 17,000 soil/rock segments, and 18,000 vegetation segments were used for training. All the models were run and analyzed individually. In the first classification phase, three land-cover types (i.e., water, soil/rock, and vegetation) were classified, while a second classification phase concentrated on distinguishing different types of vegetation through the use of field-verified samples that were obtained from areas around the lakes.

The output produced after classification was exported and compared among classifiers. The highest classification accuracy was obtained using the Bayesian classifier, particularly for spectral separation of similar types of vegetation in complex terrain.

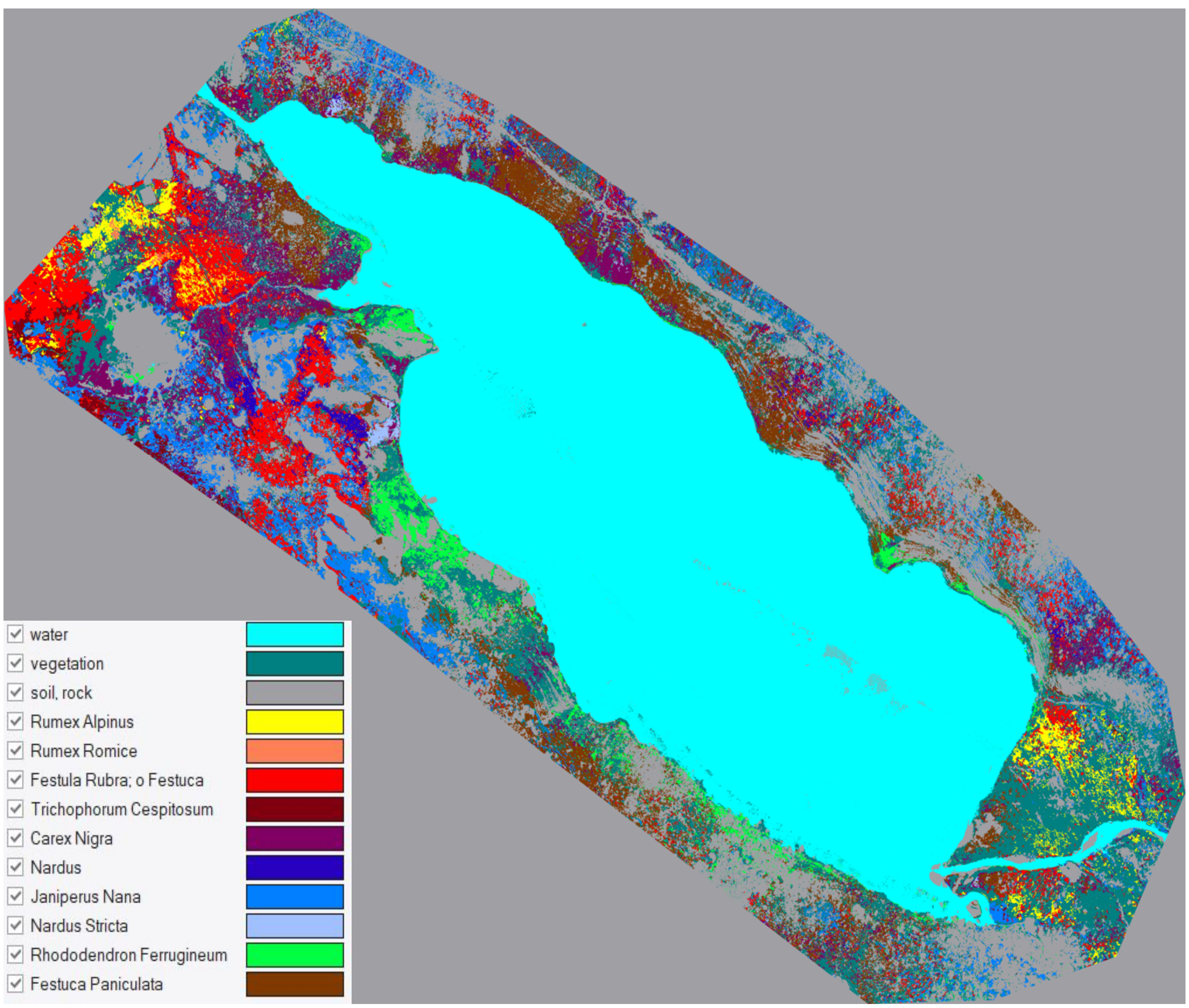

Figure 19-Bayesian classification for Vej Del Bouc Lake

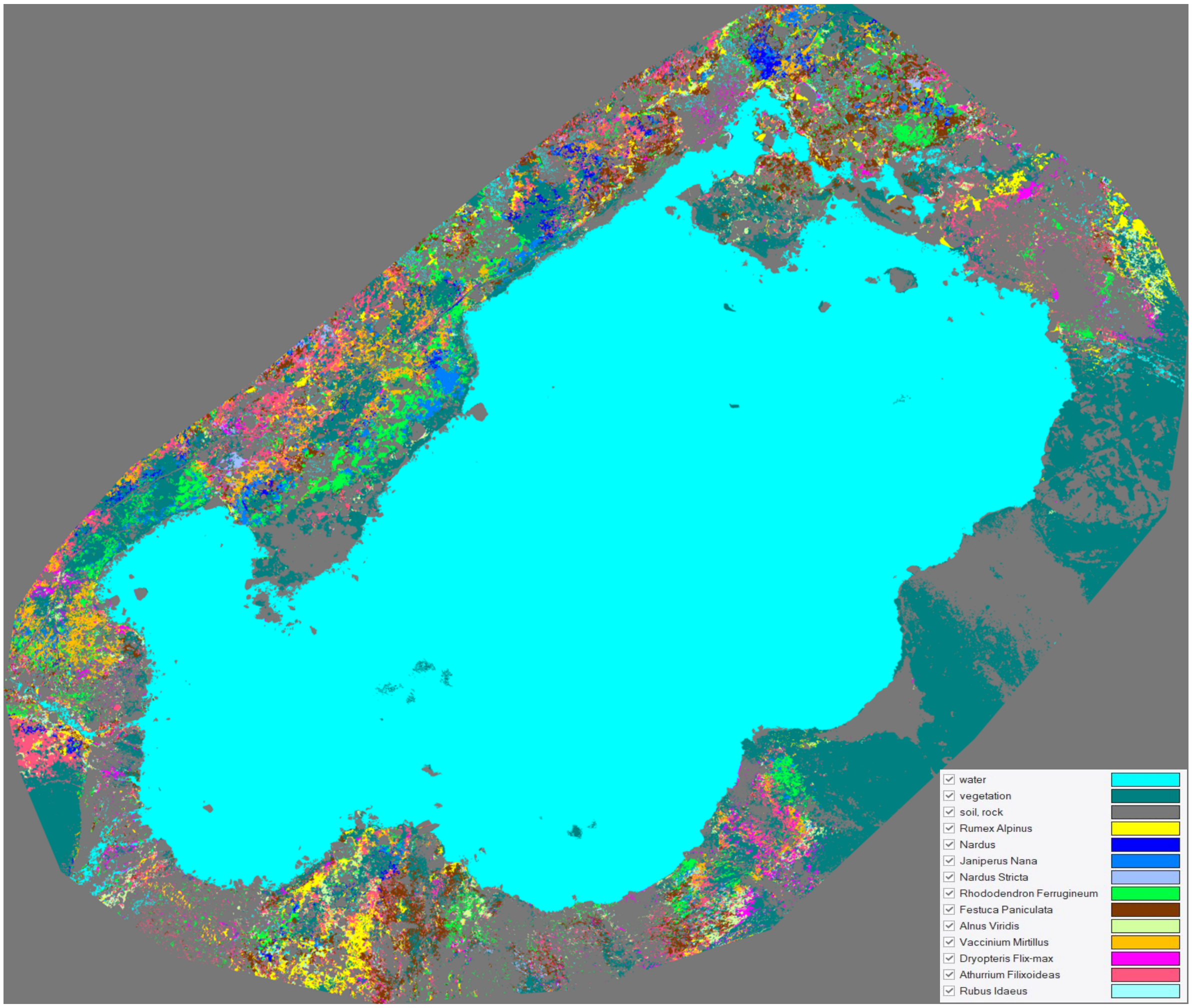

Figure 20-Bayesian classification for Brocan Lake

The accuracy of UAV-based estimates for overall classification was above 90%, and the Bayesian model always performed better than the other methods in segment purity and spatial coherence. Some remaining misclassifications occurred primarily in shadowed areas or anomalous vegetation–snow transitions at high elevations, which could be manually edited.

4.3 Classification Results Overview

The following section describes the ultimate land cover classification outcomes: which is a produced independently from Sentinel-2 satellite imagery image pre-processed using GEE-to-derived orthophotos based products using UAV orthophotos using GEE satellite imagery pre-processed from and classified in GEE and orthophotos classified in eCognition Developer and employing different machine learning algorithms via these two production lines. There was no attempt in comparing the two datasets directly, but in unified classification so that the land cover interpretation remained consistent. The classification legend involved five classes: Open Water, Dense Vegetation, Sparse Vegetation, Bare Soil/Rock, Snow/Shadow (masked). This common schema was used for the analysis and the interpretation of the broad-scale and fine-scale results on the same ecological model.

In satellite imagery, the classification was carried out through the Random Forest algorithm over the Sentinel-2 images of 2017–2024 referring to the summer months of June, August and September. These time windows were chosen in order to reflect the seasonal variations of vegetation and hydrological state in the alpine landscape. The resultant maps were used as a spatio-temporal snapshot of the land cover progression in the study site and resulted at a spatial resolution of 10 m. Such an increase is consistently seen in the NDVI (Vegetation activity) maximum, which already occurs in August, in the growing season and then declines in September. Water bodies extent estimated by NDWI varied across years, which reductions were clearly evidenced during dry years, such as in 2022 (Figure 7C). The maps also showed a slow upward creep of vegetation belts, especially at higher altitudes, consistent with the continued retreat of glaciers and a warming climate. The accuracy of classification varied between circa 85 and 92%, depending on atmospheric conditions and quality of scenes, and was validated by comparison with high resolution UAV based orthophotos.

For UAV-based images, object-based image analysis was conducted in eCognition. Band-separated orthophotos were subdivided by means of a multiresolution technique, a series of spectral indices (NDVI, NDWI, EVI and SAVI) were calculated within the software environment in order to assist in its classification. Five supervised machine algorithms were performed: Bayesian, Random Forest, SVM, k-NN and Decision Tree. We utilized a large training set that included 20,000 segments of water, 17,000 segments of soil/rock and 18,000 segments of vegetation which encompassed a broad spectrum of spectral and spatial variability across both lakes and their surrounding terrain.

Of the classifiers, the Bayesian rule classifier consistently produced the highest overall accuracy (>94%) but performed especially well in the delineation of environmentally similar vegetation classes in rugged terrain. Also, Random Forest and SVM gave good results, obtaining an accuracy of 91%–93%. If we compare with KNN and decision Tree which had a worse accuracy between the 88% and 91%. Most misclassifications were related to shadowed surfaces and the borders between vegetation and snow, particularly at high elevation and in north aspects. Manual interventions were performed in the post-processing.

In general, classification results produced by GEE and eCogntion, which were obtained independently but used the same land cover legend, were consistent in the representation of main environmental drivers in the study area. The satellite-based maps yielded strong temporal reference to identifying major changes in the land cover, but the UAV-based maps offered highly detailed and high-resolution images necessary to ecological mapping and site-specific vegetation assessments. As a whole these products are a complete and scalable package to monitor alpine ecosystems for a range of climatic and anthropogenic pressures.

5 Discussion

This investigation demonstrates the success of multi-source object-based remote sensing classification in alpine vegetation and land cover mapping. With the combination of medium-resolution Sentinel-2 satellite images and ultra-high-resolution UAV orthophotos, we succeeded in meeting the spatial and temporal dimensions of ecological monitoring in mountainous areas. The integration of GEE for long-term processing of satellite data together with eCognition Developer for fine-scale classification of UAV-derived data enabled the achievement of a complete framework for the rocky environment of the Maritime Alps.

The classification results produced by both platforms were derived using the same three category classification scheme that features open water, vegetation, soil or rock. This assessment, based on Sentinel-2 imagery with the Random Forest (RF) classifier, provided a valuable temporal panorama of dynamic land cover between 2017 and 2024. This allowed us to document phenological dynamics (e.g., decline in lake surface area in the drier 2022, seasonal NDVI trends, slow upward migration of vegetation belts in the wake of glacial retreats and warming temperatures). Overall classification accuracy rates, compared with UAV-based orthophotos, varied between 85% and 92%.

The OBIA-based classification derived from UAV was found to have better spatial accuracy and more detailed discrimination of vegetation. Five classification algorithms were evaluated: Bayesian, Random Forest, SVM, kNN, and Decision Tree. The Bayesian classifier performed best among them, all yielding accuracies over 94%. Its performance was especially strong in complex terrain or for spectral discrimination of vegetation classes that are spectrally similar, such as transient grassland types or mixed sedge communities. This is likely due to the probabilistic nature of the Bayesian model, which handles class uncertainty and overlapping spectral features more effectively than ensemble or kernel-based techniques. We provide a graphic overview of the classifiers' performance in Figure 21, which compares overall accuracies and class-specific ones for each of the algorithms.

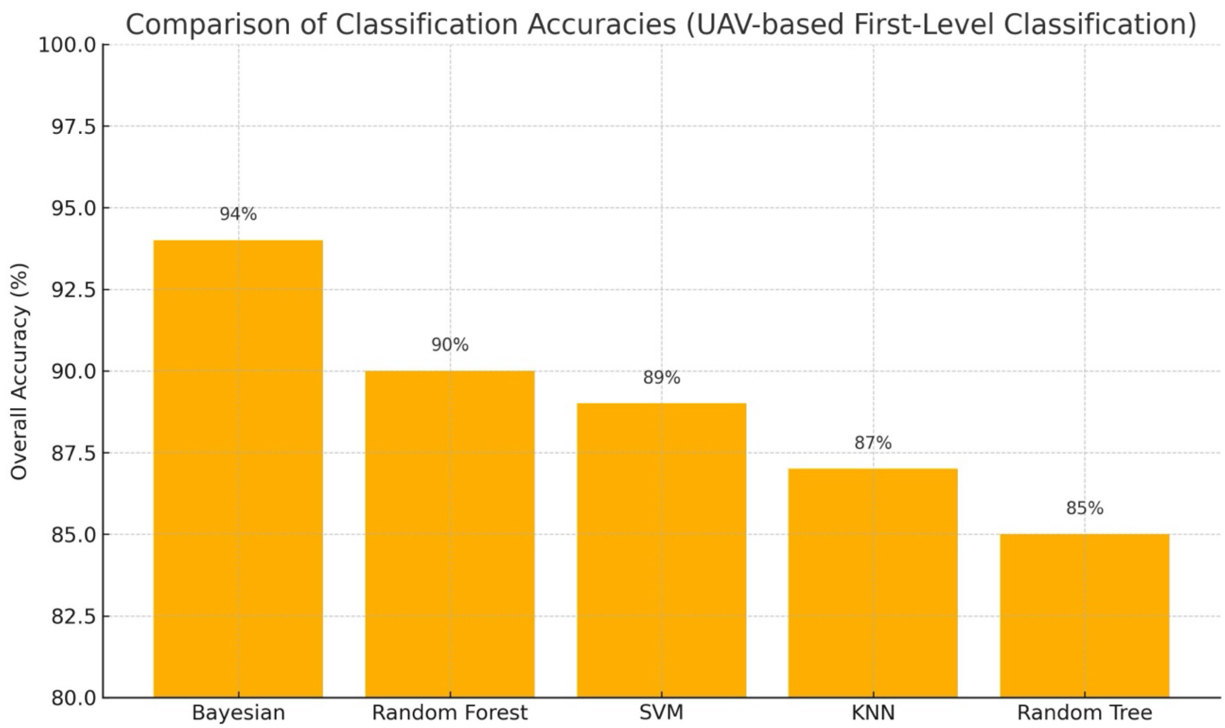

Figure 21-Comparison of classification accuracies

Although in general the UAV workflow performed well, some problems occurred during data acquisition and processing. In a few of the north-facing or steeper slopes, shading led to underestimation of vegetation reflectance, with the consequence of mistakenly assigning forested areas as exposed soil or even open water. This can visually be seen in Figure 22 and is shown to produce shadow misclassification effects near Lago Brocan.

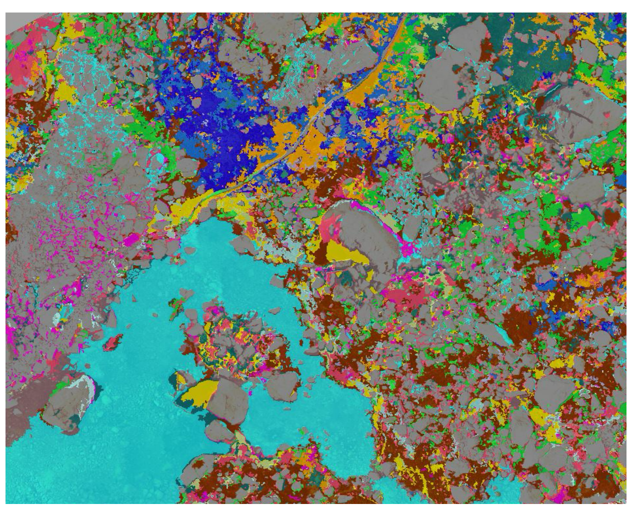

Figure 22- shadow misclassification effects

In addition, some specific parts of the orthophoto mosaic (particularly in the area close to Lago Brocan) had visually degraded quality, possibly due to suboptimal flying conditions. Motion blur caused by wind-induced instability during data acquisition could have limited the quality of the final orthoimages, and on a few strips the overlap between the images was lower than expected, weakening Metashape's ability to produce clean, radiometrically consistent products.These inconsistencies resulted in local seams and striping in the orthomosaics and potentially affected segments in the object-based classification.

Apart from the orthophoto quality, minor errors in co-registering spectral bands were found on several image tiles. These spatial inconsistencies, presumably due to poor or missing tie points between either the red band and other bands or across the entire image, led to spectral discontinuities along the object edges. Although the problem was partly alleviated by the introduction of ground control points (GCPs) and manual correction, there was still a certain amount of misalignment that could have decreased classification accuracy at object edges.

Also of vital importance was the limited availability of ground-truth data. Field validation in the two lakes was restricted to specific zones around both sites because of the rough terrain, the presence of snow cover, and limited accessibility. While a large number of training and validation examples were manually labeled from UAV imagery, some bias likely resulted from the small number of in-situ vegetation observations, particularly in the less accessible or more ecologically significant parts. Furthermore, in-situ water level measurements were absent for quantitative validation of lake area changes derived from NDWI.

Several suggestions to enhance the methodology of future studies are proposed. First, UAV flight planning should prioritize stable weather conditions, high forward and sidelap (ideally $\geq$ 80%), and lower sun angles to mitigate shadowing. Increasing the accuracy of RTK or PPK georeferencing and expanding the number of GCPs would lead to better image alignment and reduced registration errors. In addition, topographic correction methods or shadow-invariant spectral indices are potential tools to reduce classification errors in low-illumination areas. From a modeling viewpoint, hybrid solutions that integrate Bayesian probabilistic inference with ensemble approaches such as RF stacking may achieve better classification performance, especially in data-scarce settings. Finally, field campaigns could be extended to include portable spectroradiometry, canopy structure surveys, or UAV LiDAR in order to generate validation data for a more reliable and ecologically oriented classification.

In conclusion, the combination of UAV and satellite data implemented in an object-based framework proved powerful for vegetation classification and landscape monitoring in alpine settings. The superior result of the Bayesian classifier, particularly in spatially complex surfaces, provides a critical perspective that runs counter to the current tendency in remote sensing to favor more computationally intensive methods. These findings underscore the importance of selecting classification approaches based on ecological context and data quality, rather than algorithm popularity. Although logistical and technical challenges, such as shadows, band misalignment, and limited validation data, present constraints, they also offer a clear opportunity for methodological improvement in future alpine observation programs.

6 Conclusion

This study has developed and demonstrated the effectiveness of a multiscale remote-sensing approach, combining centimetric UAV multispectral imagery with the multi-temporal record of Sentinel-2 for mapping vegetation and land cover types in alpine environments at an improved level of accuracy. Focusing on Lago Vej del Bouc and Lago Brocan, the study illustrates that the combination of ultra-fine spatial resolution and multi-year temporal extent is a critical requirement for environmental monitoring in alpine headwaters.

Utilising an object-based image analysis methodology in eCognition, the study leveraged spatial, spectral, and contextual information to reduce the misclassifications usually associated with shadows, spectral mixture, and fragmented land-cover mosaics. A hierarchical approach that initially separated water, soil/rock, and vegetation classes, and then further refined vegetation classes with ground-based truthing, produced a combination of thematic accuracy and ecological breadth.

Comparison of the five supervised algorithms revealed a clear and unexpected winner: the Bayesian classifier, which significantly outperformed Random Forest, SVM, k-Nearest Neighbors, and Random Tree at both the broad and fine thematic levels. Its "fuzzy" handling of class uncertainty was particularly useful on slopes where vegetation communities overlapped, and spectral signatures converged. This result emphasizes that the choice of algorithm should be driven by data structure and landscape complexity, and not simply by convention.

The band-separated processing of UAV imagery in Agisoft Metashape turned out to be crucial. With centimeter-level spatial resolution, narrow riparian strips, semi-aquatic sedge patches, and early-successional talus vegetation were accurately segmented—features that remained sub-pixel in Sentinel-2 imagery. Sentinel-2's two-week revisit cycle between 2017 and 2024, on the other hand, provided valuable temporal context: through a timeseries of NDVI, NDWI, EVI, and SAVI, we observed seasonal greening, variations in water levels, and the continuous upward movement of the vegetation belt associated with glacial retreat and warming temperatures.

Limitations remain. Field validation was constrained by snow, steep topography, and limited accessibility; and some orthophoto strips were affected by motion blur and co-registration error. Nevertheless, the synergistic capabilities of UAV detail and satellite continuity produced a robust, scalable solution that can be adapted and applied to other high-relief ecosystems.

In general, this thesis delivers a transferable framework for alpine land-cover mapping, demonstrating that object-based delineation, probabilistic classification, and sensor fusion jointly contribute to the improvement of ecological surveillance. With landscape transformations occurring at high elevations at an unprecedented rate due to climate change, such integrative approaches will be essential for conservation planning, resource management, and biodiversity protection in mountain regions globally.

References

[1] C. Körner, “Concepts in Alpine Plant Ecology,” *Plants*, vol. 12, no. 14, Art. no. 14, Jan. 2023, doi: 10.3390/plants12142666.

[2] C. Körner, “Coldest places on earth with angiosperm plant life,” *Alp. Bot.*, vol. 121, no. 1, pp. 11–22, Apr. 2011, doi: 10.1007/s00035-011-0089-1.

[3] B. Johnson and L. Ma, “Image Segmentation and Object-Based Image Analysis for Environmental Monitoring: Recent Areas of Interest, Researchers’ Views on the Future Priorities,” *Remote Sens.*, vol. 12, p. 1772, Jun. 2020, doi: 10.3390/rs12111772.

[4] M. Beniston *et al.*, “The European mountain cryosphere: a review of its current state, trends, and future challenges,” *The Cryosphere*, vol. 12, no. 2, pp. 759–794, Mar. 2018, doi: 10.5194/tc-12-759-2018.

[5] W. Turner, S. Spector, N. Gardiner, M. Fladeland, E. Sterling, and M. Steininger, “Remote sensing for biodiversity science and conservation,” *Trends Ecol. Evol.*, vol. 18, no. 6, pp. 306–314, Jun. 2003, doi: 10.1016/s0169-5347(03)00070-3.

[6] I. Dronova, “Object-Based Image Analysis in Wetland Research: A Review,” *Remote Sens.*, vol. 7, no. 5, Art. no. 5, May 2015, doi: 10.3390/rs70506380.

[7] M. Drusch *et al.*, “Sentinel-2: ESA’s Optical High-Resolution Mission for GMES Operational Services,” *Remote Sens. Environ.*, vol. 120, pp. 25–36, May 2012, doi: 10.1016/j.rse.2011.11.026.

[8] E. Salamí, C. Barrado, and E. Pastor, “UAV Flight Experiments Applied to the Remote Sensing of Vegetated Areas,” *Remote Sens.*, vol. 6, no. 11, Art. no. 11, Nov. 2014, doi: 10.3390/rs61111051.

[9] D. Lu and Q. Weng, “A survey of image classification methods and techniques for improving classification performance,” *Int. J. Remote Sens.*, vol. 28, no. 5, pp. 823–870, Mar. 2007, doi: 10.1080/01431160600746456.

[10] T. Blaschke, “Object based image analysis for remote sensing,” *ISPRS J. Photogramm. Remote Sens.*, vol. 65, no. 1, pp. 2–16, Jan. 2010, doi: 10.1016/j.isprsjprs.2009.06.004.

[11] M. Belgiu and L. Drăguţ, “Random forest in remote sensing: A review of applications and future directions,” *ISPRS J. Photogramm. Remote Sens.*, vol. 114, pp. 24–31, Apr. 2016, doi: 10.1016/j.isprsjprs.2016.01.011.

[12] B. Gao, “NDWI—A normalized difference water index for remote sensing of vegetation liquid water from space,” *Remote Sens. Environ.*, vol. 58, no. 3, pp. 257–266, Dec. 1996, doi: 10.1016/S0034-4257(96)00067-3.

[13] J. Dozier and S. G. Warren, “Effect of viewing angle on the infrared brightness temperature of snow,” *Water Resour. Res.*, vol. 18, no. 5, pp. 1424–1434, 1982, doi: 10.1029/WR018i005p01424.

[14] A. Guisan *et al.*, “Using Niche-Based Models to Improve the Sampling of Rare Species,” *Conserv. Biol.*, vol. 20, no. 2, pp. 501–511, 2006, doi: 10.1111/j.1523-1739.2006.00354.x.

[15] M. Immitzer, F. Vuolo, and C. Atzberger, “First Experience with Sentinel-2 Data for Crop and Tree Species Classifications in Central Europe,” *Remote Sens.*, vol. 8, no. 3, Art. no. 3, Mar. 2016, doi: 10.3390/rs8030166.

[16] F. E. Fassnacht *et al.*, “Review of studies on tree species classification from remotely sensed data,” *Remote Sens. Environ.*, vol. 186, pp. 64–87, Dec. 2016, doi: 10.1016/j.rse.2016.08.013.

[17] C. J. Tucker, “Red and photographic infrared linear combinations for monitoring vegetation,” *Remote Sens. Environ.*, vol. 8, no. 2, pp. 127–150, May 1979, doi: 10.1016/0034-4257(79)90013-0.
[18] S. K. McFEETERS, “The use of the Normalized Difference Water Index (NDWI) in the delineation of open water features,” *Int. J. Remote Sens.*, vol. 17, no. 7, pp. 1425–1432, May 1996, doi: 10.1080/01431169608948714.
[19] “Geo-Object-Based Vegetation Mapping via Machine Learning Methods with an Intelligent Sample Collection Scheme: A Case Study of Taibai Mountain, China.” Accessed: Jul. 13, 2025. [Online]. Available: https://www.mdpi.com/2072-4292/13/2/249
[20] H. Aasen, A. Burkart, A. Bolten, and G. Bareth, “Generating 3D hyperspectral information with lightweight UAV snapshot cameras for vegetation monitoring: From camera calibration to quality assurance,” *ISPRS J. Photogramm. Remote Sens.*, vol. 108, pp. 245–259, Oct. 2015, doi: 10.1016/j.isprsjprs.2015.08.002.
[21] M. Pal and P. M. Mather, “Support vector machines for classification in remote sensing,” *Int. J. Remote Sens.*, vol. 26, no. 5, pp. 1007–1011, Mar. 2005, doi: 10.1080/01431160512331314083.
[22] L. Breiman, “Random Forests,” *Mach. Learn.*, vol. 45, no. 1, pp. 5–32, Oct. 2001, doi: 10.1023/A:1010933404324.
[23] Y. Xie, Z. Sha, and M. Yu, “Remote sensing imagery in vegetation mapping: a review,” *J. Plant Ecol.*, vol. 1, no. 1, pp. 9–23, Mar. 2008, doi: 10.1093/jpe/rtm005.
[24] C. Zhang and J. M. Kovacs, “The application of small unmanned aerial systems for precision agriculture: a review,” *Precis. Agric.*, vol. 13, no. 6, pp. 693–712, Dec. 2012, doi: 10.1007/s11119-012-9274-5.
[25] M. Immitzer, C. Atzberger, and T. Koukal, “Tree Species Classification with Random Forest Using Very High Spatial Resolution 8-Band WorldView-2 Satellite Data,” *Remote Sens.*, vol. 4, no. 9, Art. no. 9, Sep. 2012, doi: 10.3390/rs4092661.
[26] Q. Weng, “Remote sensing of impervious surfaces in the urban areas: Requirements, methods, and trends,” *Remote Sens. Environ.*, vol. 117, pp. 34–49, Feb. 2012, doi: 10.1016/j.rse.2011.02.030.
[27] A. R. Huete, “A soil-adjusted vegetation index (SAVI),” *Remote Sens. Environ.*, vol. 25, no. 3, pp. 295–309, Aug. 1988, doi: 10.1016/0034-4257(88)90106-X.
[28] X. Gao, A. R. Huete, W. Ni, and T. Miura, “Optical–Biophysical Relationships of Vegetation Spectra without Background Contamination,” *Remote Sens. Environ.*, vol. 74, no. 3, pp. 609–620, Dec. 2000, doi: 10.1016/S0034-4257(00)00150-4.
[29] H. Xu, “Modification of normalised difference water index (NDWI) to enhance open water features in remotely sensed imagery,” *Int. J. Remote Sens.*, vol. 27, no. 14, pp. 3025–3033, Jul. 2006, doi: 10.1080/01431160600589179.
[30] J. Xue and B. Su, “Significant Remote Sensing Vegetation Indices: A Review of Developments and Applications,” *J. Sens.*, vol. 2017, no. 1, p. 1353691, 2017, doi: 10.1155/2017/1353691.
[31] F. Mena, D. Arenas, M. Nuske, and A. Dengel, “Common Practices and Taxonomy in Deep Multiview Fusion for Remote Sensing Applications,” *IEEE J. Sel. Top. Appl. Earth Obs. Remote Sens.*, vol. 17, pp. 4797–4818, 2024, doi: 10.1109/JSTARS.2024.3361556.
[32] O. Stolarski, H. Fraga, J. J. Sousa, and L. Pádua, “Synergistic Use of Sentinel-2 and UAV Multispectral Data to Improve and Optimize Viticulture Management,” *Drones*, vol. 6, no. 11, Art. no. 11, Nov. 2022, doi: 10.3390/drones6110366.

[33] P. M. Teillet, B. Guindon, and D. G. Goodenough, "On the Slope-Aspect Correction of Multispectral Scanner Data," *Can. J. Remote Sens.*, vol. 8, no. 2, pp. 84–106, Dec. 1982, doi: 10.1080/07038992.1982.10855028.

[34] X. Zhang *et al.*, "Monitoring vegetation phenology using MODIS," *Remote Sens. Environ.*, vol. 84, no. 3, pp. 471–475, Mar. 2003, doi: 10.1016/S0034-4257(02)00135-9.

[35] D. J. Lary, A. H. Alavi, A. H. Gandomi, and A. L. Walker, "Machine learning in geosciences and remote sensing," *Geosci. Front.*, vol. 7, no. 1, pp. 3–10, Jan. 2016, doi: 10.1016/j.gsf.2015.07.003.

[36] G. Mountrakis, J. Im, and C. Ogole, "Support vector machines in remote sensing: A review," *ISPRS J. Photogramm. Remote Sens.*, vol. 66, no. 3, pp. 247–259, May 2011, doi: 10.1016/j.isprsjprs.2010.11.001.

[37] X. X. Zhu *et al.*, "Deep Learning in Remote Sensing: A Comprehensive Review and List of Resources," *IEEE Geosci. Remote Sens. Mag.*, vol. 5, no. 4, pp. 8–36, Dec. 2017, doi: 10.1109/MGRS.2017.2762307.

[38] L. Ma, Y. Liu, X. Zhang, Y. Ye, G. Yin, and B. A. Johnson, "Deep learning in remote sensing applications: A meta-analysis and review," *ISPRS J. Photogramm. Remote Sens.*, vol. 152, pp. 166–177, Jun. 2019, doi: 10.1016/j.isprsjprs.2019.04.015.

[39] T. Kattenborn, J. Eichel, and F. E. Fassnacht, "Convolutional Neural Networks enable efficient, accurate and fine-grained segmentation of plant species and communities from high-resolution UAV imagery," *Sci. Rep.*, vol. 9, no. 1, p. 17656, Nov. 2019, doi: 10.1038/s41598-019-53797-9.

[40] J. E. Ball, D. T. Anderson, and C. S. C. Sr, "Comprehensive survey of deep learning in remote sensing: theories, tools, and challenges for the community," *J. Appl. Remote Sens.*, vol. 11, no. 4, p. 042609, Sep. 2017, doi: 10.1117/1.JRS.11.042609.

Acknowledgment

I would like to express my deepest gratitude to Prof. Francesca Matrone and Eng. Alessandra Spadaro for their exceptional guidance, encouragement, and continuous support throughout this thesis. Their expertise, patience, and thoughtful feedback were instrumental in shaping the direction and quality of my research.

I am sincerely thankful to the Politecnico di Torino Geomatics Laboratory for providing the UAV data and technical support during the fieldwork, and to the ACLIMO project team, including collaborators from the APAM (Management Authority of the Protected Areas of the Maritime Alps), for their contributions and for making this interdisciplinary research possible.

I owe special thanks to my family, whose love, sacrifices, and unwavering belief in me have been the foundation of my academic journey. Their support gave me the strength to overcome challenges and pursue my goals far from home.

I dedicate this work to my homeland, Iran, and to its people, who continue to face hardship with strength and resilience. In these difficult times, as my country endures the pain and uncertainty of conflict, I offer this academic effort as a symbol of hope and a small contribution to a brighter, more peaceful future. My thoughts and best wishes remain with those who are suffering, and with all who continue to believe in the power of knowledge, unity, and peace.